

1 Exotic tree plantations in the Chilean Coastal Range: Balancing
2 effects of discrete disturbances, connectivity and a persistent
3 drought on catchment erosion

4

5

June 28, 2022

6 Abstract

7 The Coastal Range in the Mediterranean segment of the Chilean active margin is a soil mantled landscape able
8 to store fresh water and potentially support a biodiverse native forest. In this landscape, human intervention
9 has been increasing soil erosion for ~ 200 yr, with the last ~ 45 yr experiencing intensive management of exotic
10 tree plantations. Such intense forest management practices come along with rotational cycles as short as 9-25
11 yrs, the construction of dense forest road networks, and the fostering of wildfire susceptibility due to the high
12 amounts of fuel provided by dense plantation stands. Here we first compare decadal-scale catchment erosion
13 rates from suspended sediment loads with a 10^4 -years-scale catchment erosion rate estimated from detritic
14 ^{10}Be . We then explore these erosion rates against the effects of discrete disturbances and hydroclimatic
15 trends. Erosion rates are similar on both time scales, i.e. 0.018 ± 0.005 mm/yr and 0.024 ± 0.004 mm/yr,
16 respectively. Recent human-made disturbances include logging operations during each season and a dense
17 network of forestry roads, which increase structural sediment connectivity. Other disturbances include the
18 2010 M_w 8.8 Maule earthquake, and two widespread wildfires in 2015 and 2017. A decrease in suspended
19 sediment load is observed during the wet seasons for the period 1986-2018 coinciding with a decline in several
20 hydroclimatic parameters. The low 10^4 -years erosion rate agrees with a landscape dominated by slow soil
21 creep. The low 10-years-scale erosion rate and the decrease in suspended sediments, however, conflicts
22 with both the observed disturbances and increased structural (sediment) connectivity. These observations
23 suggest that, either suspended sediment loads and, thus, catchment erosion, are underestimated, and/or
24 that decennial sediment detachment and transport were smeared by decreasing rainfall and streamflow.
25 Our findings indicate that human-made disturbances and hydrometeorologic trends may result in opposite,
26 partially offsetting effects on recent sediment transport.

27 Introduction

28 Over 75% of Earth's ice-free land has been altered by humans (Ellis and Ramankutty, 2008), with severe
29 consequences for sediment transport during the Anthropocene (Syvitski et al., 2022). Land Use and Land
30 Cover Changes (LULCC) are important in increasing soil erosion (Borrelli et al., 2020). Human-made forests
31 – or better, tree plantations (DellaSala, 2020) – are frequently disturbed by logging and the implementation
32 of forestry roads. Such disturbances may intensify soil erosion (e.g., Schuller et al., 2013; Sidle and Ziegler,
33 2012), alike as heavy machinery traffic (e.g., Malmer and Grip, 1990), wildfires and terracing (e.g., Martins
34 et al., 2013). Short rotational cycles, i.e. the period between planting, harvesting, and replanting of tree
35 plantations, also change hillslope stability by cycles of root strength decay and recovery, which in turn
36 promote landsliding and debris flows (Imaizumi et al., 2008; Montgomery et al., 2000). Ultimately, all such
37 processes may modify sediment trajectories and storage on hillslopes and along rivers (Wainwright et al.,
38 2011) with long-lasting impacts on sediment yields for periods of 10-100 years (Moody and Martin, 2009;
39 Bladon et al., 2014).

40 The Chilean Coastal Range (CCR) in its Mediterranean section (35 - 37.5° S) is a landscape of gentle
41 and largely convex hillslopes. Here, forests, soils and water are closely coupled (Galleguillos et al., 2021).
42 This morphology results from relatively slow denudation rates by soil creep on regolith-mantled landscapes
43 (Roering et al., 2007), yet modified by the underlying bedrock (Gabet et al., 2021). Detrital ^{10}Be denudation
44 rates in this landscape point to between 0.02 and 0.05 mm/yr (Carretier et al., 2018), which are low compared

45 to the global data for catchments of similar size (Covault et al., 2013). Currently, the remnants of secondary
 46 native forest stand on soils as thick as 2 m (Soto et al., 2019), suggesting such minimum soil depths under
 47 undisturbed conditions. In the absence of snow storage, these soils form a major fresh water supply along
 48 the Mediterranean CCR, which many rural communities rely on. Thus, decision-making regarding land
 49 management is strategic for the resilience of these communities (e.g., Gimeno et al., 2022), specially under
 50 recent (Garreaud et al., 2020) and projected (IPCC, 2021) conditions of water scarcity.

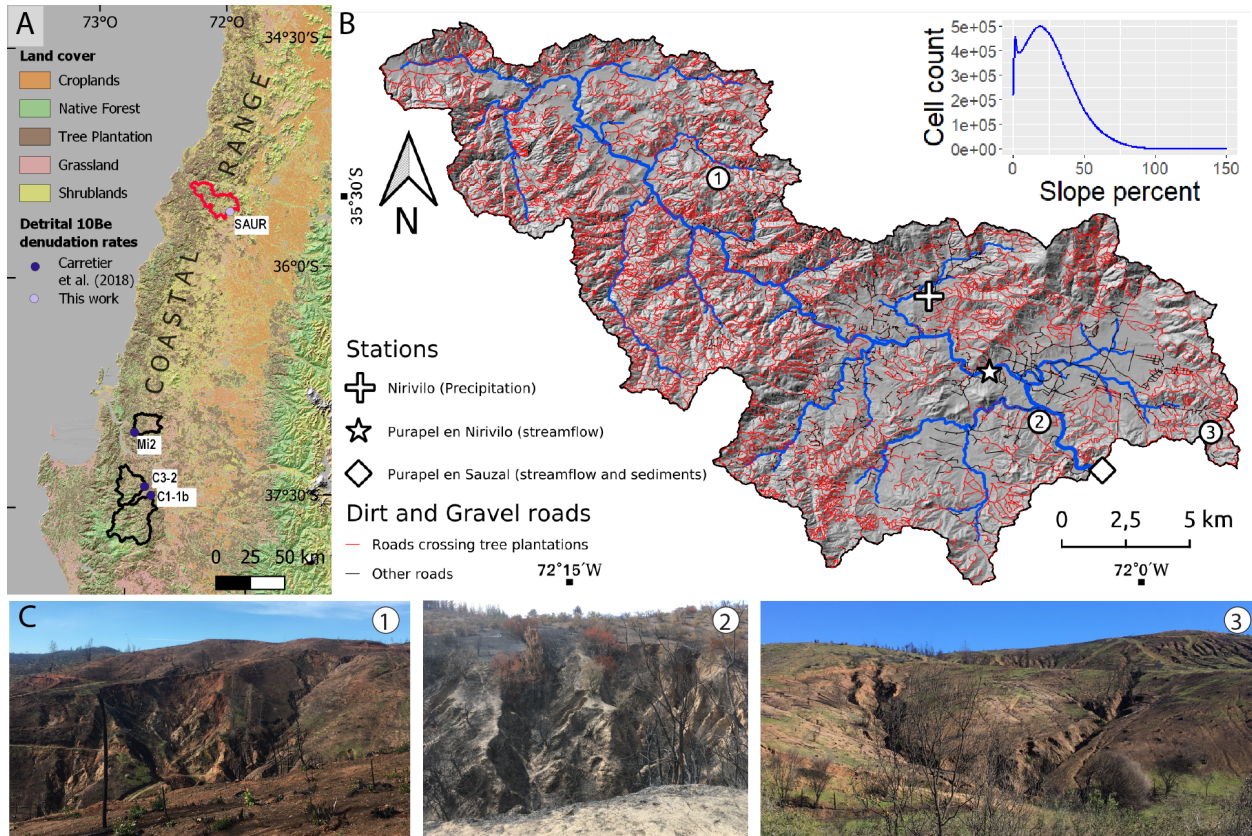


Figure 1: Study region. A. Land cover in the Coastal Range (Zhao et al., 2016) and detrital ^{10}Be denudation rates of table 1. B. Purapel catchment. All the detected forestry roads intersecting tree plantations and the position of photos in C are shown. Elevation data comes from a 5-m resolution LiDAR DTM obtained in 2009. C. Photos captured on hillslopes of Purapel catchment.

Name	Denudat. rate (mm/yr)	Denudat. rate unc. (mm/yr)	Char. time (kyr)	Lat	Lon	Catch. area (km ²)	Analyzed grain size (mm)	[^{10}Be] (at/g)	[^{10}Be] unc. (at/g)	Standard material	Source
SAUR	0.024	0.004	25	-35.6197	-72.0171	406	[0.5,1]	143751	5469	STD-11	This work
Mi2	0.037	0.006	16	-37.0488	-72.8614	235	[0.5,1]	93772	4280	4325	Carretier et al. (2018)
C3-2	0.039	0.007	15	-37.4052	-72.7976	357	[0.5,1]	97896	8272	4325	Carretier et al. (2018)
C1-1b	0.041	0.010	14	-37.4652	-72.7495	739	[0.5,1]	113680	20735	4325	Carretier et al. (2018)

Table 1: Detrital ^{10}Be denudation rates in the Mediterranean CCR.

51 The CCR has been experienced deforestation for more than 200 years (Armesto et al., 2010) intensifying

52 soil erosion, as it has been already recognized by Bianchi-Gundian (1947) and Chilean governments in the
53 middle of 20th century (IREN, 1965). From the beginning of 20th century, governments blamed environmen-
54 tal issues due to deforestation to promote the expansion of tree plantations (e.g., CONAF and MINAGRI,
55 2016; Pizarro et al., 2020). The most relevant transformation of land cover began with the law DL 701
56 (1974) to subsidize the forestry sector (Manushevich, 2020). This law and following political action accel-
57 erated LULCC, which in practice transformed degraded lands, shrublands and native forest into industrially
58 managed tree plantations (Heilmayr et al., 2016). From $\sim 450,000$ ha of tree plantations in 1974 (Barros,
59 2018), their spatial extent increased to at least some 2.8 ± 0.2 millions ha in 2011 (Heilmayr et al., 2016),
60 mostly within the Mediterranean CCR (Fig. 1).

61 In Chile, tree plantations are managed mostly as monocultures of fast-growing *Eucalyptus* spp or *Pinus*
62 *Radiata*. The rotation cycles are as short as 9-12 and 18-25 years, respectively (INFOR, 2004; Gerding,
63 1991). As a consequence, the CCR ranks among the highest worldwide in terms of combined forest loss and
64 gain (Hansen et al., 2013). (Hansen et al., 2013) identified tree cover, forest loss and gain from Landsat
65 imagery which in turn provide time-series of spectral metrics at each pixel. Clear-cut areas in Chilean tree
66 plantations are generally detectable at the Landsat resolution scale because the clear-cuts usually expand
67 over entire hillslopes (Fig. 2). Such practice is permitted by current Chilean law, as clear-cutting require
68 environmental impact assessments only for harvest areas ≥ 500 ha/yr or $\geq 1,000$ ha/yr in Mediterranean
69 and Temperate regions, respectively (*Artículo Primero, Título I, Artículo 3, m.1* at Chilean Law 19.300,
70 2013).

71 Tree plantations frequently are intersected by dense networks of logging roads. These roads are intended to
72 facilitate access and use of heavy forest machinery, storage and transport of timber, as well as the subsequent
73 (re-)plantation. Logged hillslopes alike logging roads are important sediment sources during storms and after
74 wet-season clear-cutting (Schuller et al., 2013, 2021; Aburto et al., 2020). For example, Aburto et al. (2020)
75 reported highest post-harvest soil loss in a catchment sustaining a one-year-old plantation. Post-harvest
76 erosion is mainly rainfall triggered (Aburto et al., 2020; Schuller et al., 2013) and after exceeding specific
77 rainfall intensity thresholds (Mohr et al., 2013). The erosional work efficacy depends on the logging season,
78 which is higher for wet season logging (Mohr et al., 2014). At the storm to yearly scale (10^{-4} - 10^0 yr), roads
79 are prime sources and routers of sediments in catchments covered by tree plantations (Schuller et al., 2013).
80 This is not surprising, since they remain bare and prone for compaction by heavy machinery transit. These
81 roads often intersect streams, which form bypasses to preferentially route sediment (Fig. 2), increasing the
82 efficacy of mass transfer within a geomorphic system or sediment connectivity (Wohl et al., 2019). In this
83 case, road networks modify the pathways of runoff and sediments, and may also modify thresholds of rainfall
84 to trigger sediment detachment and transport (for example, due to soil compaction), potentially affecting
85 the structural and functional components of sediment connectivity, as defined by Wainwright et al. (2011).
86 This shift is also relevant to constrain off-site impacts of soil erosion (Boardman et al., 2019).

87 Despite the increase in structural connectivity, sediment mobilization depends mostly on specific thresh-
88 olds of rainfall. For example, hydrologic connectivity to initiate runoff in recently logged areas required a
89 threshold of 20 mm/hr in rainfall simulations on tree plantations near Nacimiento (Mohr et al., 2013). In
90 the absence of long term records of rainfall intensities, hydro climatic trends on rainfall and streamflow are
91 relevant to interpret catchment erosion. In Central Chile (30 - 39° S), rainfall decreased at ca. 4% per decade
92 between 1960 and 2016 (Boisier et al., 2018b), culminating into an unprecedented megadrought starting 2010
93 (Garreaud et al., 2020).

94 While the erosional response of logging is largely indisputable, hydrologic responses to tree harvest are
95 ambiguous. On the one hand, logging may increase streamflow discharge in general and peak flow in particular
96 (Iroumé et al., 2006), logging may also decrease streamflow discharge due to enhanced groundwater recharge
97 immediately after logging (Mohr, 2013). The distinct responses may most likely vary with tree species
98 and age, harvest size, forestry treatment (thinning, clear cutting, replanting), riparian buffer width, and
99 especially, with the moisture storage decrease under recent drought conditions, which exacerbated declines
100 in runoff (Iroumé et al., 2021).

101 In addition to the mega-drought, recent increase in both magnitude and frequency in wildfire affects
102 relatively more tree plantations compared to alternative land cover (Bowman et al., 2019). This is likely
103 because fuel is more abundant under dense plantation cover that connect large continuous tracts of the
104 landscape. Instead, native species are more patchy (Gómez-González et al., 2017, 2018).

105 While the observed disturbances affecting the vegetation cover predict high sediment yields in rivers (e.g.,
106 Reneau et al., 2007; Brown and Krygier, 1971), the long and persistent decline in rainfall together with high
107 water demands of tree plantations is expected to reduce sediment detachment and mobilization assuming
108 fluvial transport-limited conditions. To evaluate the impacts of these opposite responses, we explore the
109 catchment scale erosion of the Purapel river (406 km² of drainage area). To this end, we combine two
110 distinct temporal scales and explore discrete disturbance events.

111 **Materials and methods**

112 **The Purapel catchment**

113 The Purapel river drains the eastern flank of the CCR. The climate is Mediterranean type. Mean annual
114 rainfall is 845 mm, and mean minimum and maximum air temperatures are 7.2 and 20.3°C, respectively,
115 and the fluvial system is exclusively pluvial (Álvarez-Garretón et al., 2018). The catchment is 406 km² and
116 dominated by metamorphic (47.5%) and granitic (44.3%) lithologies. Elevation ranges between 164 and 747
117 m a.s.l. Most hillslopes are gentle (hillslope gradients around 16%), largely convex, and incised by gullies
118 that converted this landscape into badlands (Fig. 1). CIREN (2021) classified most of those hillslopes as
119 severely affected by soil erosion. The dominant soil types are Inceptisols and Alfisols (Bonilla and Johnson,
120 2012). Soil properties are highly variable in space. Yet, soils under tree plantations are generally thinner
121 and depleted in soil organic matter. Throughout the entire soil profile, the soil bulk densities of Eucalyptus
122 (1.38 ± 0.08 to 1.58 ± 0.12 g/cm³) and Pine (1.28 ± 0.18 to 1.53 ± 0.13 g/cm³) stands are higher than
123 under native forests (0.89 ± 0.27 to 1.25 ± 0.24 g/cm³) for depths between 0 to 60 cm (Soto et al., 2019).

124 **Analysis of hydrometeorologic data**

125 Due to the high spatio-temporal variability of rainfall, we tested local trends for available hydrometeorological
126 data. To this end, we applied the Mann-Kendall test (Helsel et al., 2020) on time series of several parameters.
127 We also applied LOWESS smoothing (Cleveland, 1981) as a graphical expression of the main trends. We
128 first evaluated the completeness of the data and applied autocorrelation tests.

129 Rainfall, potential evapotranspiration and streamflow data from satellite and national stations are avail-
130 able in Mawüim (<https://mawun.cr2.cl/>) and CAMELS-CL (<https://camels.cr2.cl/>) sites. Suspended

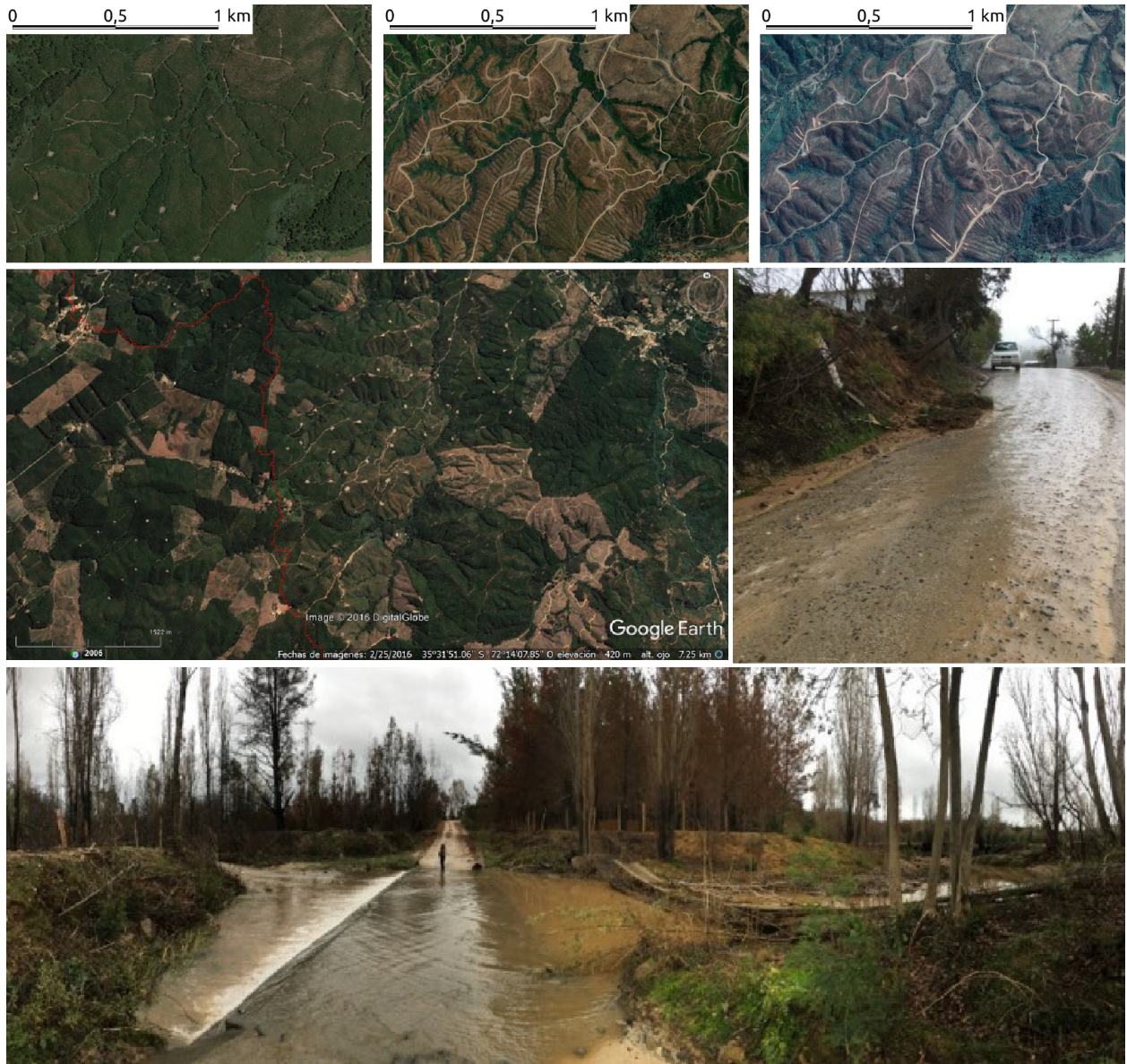


Figure 2: Details of forest roads in the Purapel catchment under different stages of the tree plantation rotational cycle and their connection to streams.

131 sediment data is available in the Chilean General Directorate of Water (DGA) site (<https://snia.mop.gob.cl/BNAConsultas/reportes>).

133 We analyzed annual and seasonal rainfall and potential evapotranspiration for several periods using
 134 both in situ (Nirivilo station) and gridded (CR2MET) data. The CR2MET product merges the ERA-
 135 Interim reanalysis, local topographic data, and the calibration with an updated national rain-gauge network
 136 (CR2MET, Boisier et al., 2018a). For annual data we excluded years with less than 330 data points and any
 137 month with less than 27 data points.

138 We also analyzed streamflow and suspended sediment loads to test for trends on annual, seasonal and
 139 monthly basis. The DGA estimated daily streamflows from single gauge stage readings using calibrated rating

140 curves. Roughly once a month, the rating curves are updated by manual current meter measurements. The
141 suspended sediment concentrations (SSC) were sampled on a daily-scale, too. All samples were obtained
142 close to the water surface in vicinity to the water stage. The samples were filtered using a cotton linter
143 cellulose paper with 80% of collection efficiency for particles larger than $0.3 \mu m$ (Advantec Qualitative Filter
144 Papers 2, written communication from DGA operator). Then, they were dried, and combusted for 2 hours
145 at 550-600°C in laboratories of the DGA (Solar, 1999).

146 The streamflow and SSC time series contain gaps. The gaps, however, are not seasonally clustered.
147 Gaps during the dry season are mostly related to ceased streamflow (personal communication from DGA
148 operator). We calculated daily suspended sediment discharge (t/day) as the product of streamflow discharge
149 (m^3/s) and suspended sediment concentration SSC (mg/l), assuming those instantaneous measurements as
150 representative of the entire day, thus converting seconds to day (Pepin et al., 2010). In addition, we calculated
151 the number of data, the percentiles and the mean value of suspended sediment discharge for single hydrologic
152 years, and the number of data and mean value of the three hydrometric parameters (streamflow, SSC and
153 sediment discharge) from monthly to annual scales.

154 For annual streamflow and suspended sediments, we excluded annual averages based on less than 185 data
155 points and/or any month with less than 15 data points. For seasonal streamflow and suspended sediments,
156 we excluded seasons with less than 60 data points. Here we define seasons as Summer (DJF), Autumn
157 (MAM), Winter (JJA) and Spring (SON). We calculated the baseflow with a standard approach using the
158 Lyne and Hollick filter (Ladson et al., 2013) on the daily streamflow at Purapel en Sauzal station. We chose
159 $\alpha=0.975$ and $n.reflected=30$ days as parameters.

160 Catchment-wide erosion rates

161 We obtained catchment-wide erosion rates for Purapel river at the gauge “Río Purapel en Sauzal” using two
162 approaches for different time scales, short-term (decadal) from suspended sediments and long-term (10^3 to
163 10^4 yrs) from detrital ^{10}Be . We calculated the long-term erosion rate to establish a benchmark to compare
164 the recent sediment yields against. In most fluvial catchments the long-term erosion rates exceed the short
165 term rates (Covault et al., 2013). This picture, however, may flip vice versa if soil erosion is high (Hewawasam
166 et al., 2003; Vanacker et al., 2007). A drawback of our approach is the fact that detrital ^{10}Be rates include
167 physical erosion and chemical weathering rates (von Blanckenburg and Willenbring, 2014), while suspended
168 sediment yields account only for physical erosion of very fine sediment (Summerfield and Hulton, 1994),
169 which excludes bedload. Thus, we regard our short-term erosion rates as minimum rates.

170 For the short-term, we calculated the mean specific sediment discharge ($t/km^2/yr$) as the annual average
171 of all records (06/1985 to 11/2018) normalized by catchment area (Pepin et al., 2010). We estimated resulting
172 erosion rate (mm/year) assuming a mean soil bulk density of $2.6 g/cm^3$ (Carretier et al., 2018).

173 For the long-term, we assume the ^{10}Be concentrations within fluvial sands are proportional for catchment-
174 wide averaged denudation rate (von Blanckenburg, 2005; Granger and Schaller, 2014). This rate integrates
175 over a characteristic timescale that is inversely proportional to the denudation rate. These timescales are
176 commonly longer than 10^3 years (Covault et al., 2013). We therefore regard the ^{10}Be derived rates as a
177 reference that largely excludes recent human disturbances but includes low frequency and high magnitude
178 erosion events (Kirchner et al., 2001). We obtained a bulk sample of fluvial sands from the active river bed
179 along a cross section close to the water stage “Río Purapel en Sauzal”. To this end, we collected sands at

180 three locations within ~ 10 m distance. We mixed all samples and sieved to a grain size fraction 0.5-1 mm.
181 The mixed sand sample was processed at the French AMS ASTER facility in CEREGE (Standard STD-11).

182 Land cover changes

183 The Purapel catchment has been experienced high rates of LULCC since back the 19th century, due to the
184 wheat extensive production boosted by the gold rush in California and Australia (Cortés et al., 2022). Later
185 on, between 1955 and 2014 tree plantations increased from (a minimum of) 10.27 (Hermosilla-Palma et al.,
186 2021) to 203.5 km² (Zhao et al., 2016). Recently, two large wildfires burned the catchment: In 2015 14% of
187 the catchment area burnt. In 2017 almost the entire catchment burnt (95%) (Tolorza et al., 2022).

188 To describe recent LULCC in this catchment, we use land cover maps both from compiled sources (1955,
189 1975 and 2017) and from our own (1986, 2000, 2005, 2010 and 2015):

- 190 • The 1955 and 1975 land cover maps of Hermosilla-Palma et al. (2021) cover the headwaters of the
191 Purapel catchment (157 km²). These maps were made interpreting the land cover from the 1:70.000
192 aerial photograph (Hycon flight) for 1955, and from the 60 m resolution Landsat-2 MMS and the
193 1:30.000 aerial photographs of 1978 (CH-30 flight) for 1975.
- 194 • We used Landsat Surface Reflectance products to identify land cover classes during dry seasons of 1986,
195 2000, 2005, 2010 and 2015. We classified unburned land cover using the Maximum Likelihood Classifier
196 (Chuvieco, 2008) which we trained and validated with 20 and 10 polygons for each class, respectively.
197 We validated the results with field observations during 2014-2015. We sub-classified burned surfaces
198 into low, moderate and severe fire according to the differences in NBR index of pre- and post- fire
199 images (thresholds $\langle 0.1 - 0.269 \rangle$, $\langle 0.27 - 0.659 \rangle$, $\langle 0.66 - 1.3 \rangle$ Key and Benson, 2006).
- 200 • The Land cover map of 2017 was made by Tolorza et al. (2022) with pre-fire Sentinel and LiDAR
201 data. Here, this classification was resampled to 30 m resolution, to be compatible with LANDSAT
202 classifications.

203 Logging roads and sediment connectivity

204 To identify changes in the structural connectivity we applied the Connectivity Index (IC , dimensionless)
205 using the weighting factor (W , dimensionless) of (Cavalli et al., 2013). IC is a semi-quantitative approach
206 to describe the degree of coupling between hillslopes and a target (for example, the stream network):

$$IC = \log_{10} \left(\frac{\overline{WS}\sqrt{A}}{\sum_i \frac{d_i}{W_i S_i}} \right) \quad (1)$$

207 , where \overline{W} and \overline{S} (m/m) are the average weighting factor and slope gradients on the upslope contributing
208 area (A , m²), respectively. d_i (m), W_i (dimensionless) and S_i (m/m) are the path length, the weighting
209 factor and the slope gradient on the i th cell in downslope towards a target.

210 W is calculated from a DTM to account for the effect of topographic roughness. The Roughness Index
211 (RI , m) is the standard deviation of the residual topography. The residual topography referees to the

212 difference between the original DTM and a smoothed version obtained by averaging DTM values on a 5×5
 213 ($=25$) cell moving window:

$$RI = \sqrt{\frac{\sum_i^{25} (x_i - x_m)^2}{25}} \quad (2)$$

214 , where x_i (m) is the value of one specific cell of the residual topography within the moving window, and x_m
 215 (m) is the mean of all 25 window cells. The weighting factor is calculated as:

$$W = 1 - \frac{RI}{RI_{max}} \quad (3)$$

216 , where RI_{max} is the maximum value of RI in the study area.

217 We quantified changes in sediment connectivity due to the forestry roads, RC , as

$$RC = IC_{rs} - IC_s \quad (4)$$

218 , where the subscripts s and rs refer to the stream network and and to the stream network including roads.
 219 We fed the model with a mapped forestry road network obtained from images available in the OpenLayers
 220 plugin of QGIS and post-2017-fire Sentinel compositions.

221 Disturbances in vegetation

222 We used the Breaks For Additive Season and Trend algorithm (BFAST, Verbesselt et al., 2010) on a LAND-
 223 SAT collection to detect disturbances in vegetation at the pixel scale, i.e. ≥ 30 m. In the Purapel catchment,
 224 disturbances > 30 m are mostly due to wildfires and/or clear-cuts. Such disturbances lean on the seasonal
 225 behavior of the NDVI index on a time series of LANDSAT surface reflectance (Level 2, Collection 2, Tier
 226 1) for the period from 09/1999 to 10/2021. Clouds were filtered using the QA band band which uses the
 227 CFMask algorithm (Foga et al., 2017). We used the same parameter set as Cabezas and Fassnacht (2018),
 228 namely the threshold value for disturbances set to 93 manually labeled reference polygons with fire events,
 229 clear-cuts and constant tree-cover. It's worth mentioning, that we applied a sieve filter to the results. Hence,
 230 only disturbances greater than 1 ha were considered. We trained the algorithm with the Landsat time se-
 231 ries of 1999 to 2001. Given the disturbance regime of Purapel catchment (two large wildfires and possible
 232 loggings each 9 to 25 years) we run BFAST anticipating three possible breaks for the period 2002-2021.

233 Results

234 Hydro climatic trends

235 At the annual scale at Nirivilo rainfall station, most data of the period 1962-2015 passed our completeness
 236 assessment criteria (53 of 54 years). In the case of CR2MET, the longest period analyzed here is 1979-2019.
 237 Judging from Mann-Kendall tests and LOWESS smoothing, we did not find a single trend for the longest
 238 interval of records (1962-2015). For the period after 1979, we see decreasing non-monotonic trends for
 239 rainfall both at Nirivilo station and for CR2MET product. That decrease is steeper for 2000-2019, but less
 240 pronounced for intermediate intervals such as 1986-2018. During 1986-2018, however, a decrease in seasonal
 241 rainfall is observed for Autumn, at the beginning of the hydrologic year (Fig. 3). Generally, the Aridity

242 Index (AI) follows similar decreasing trends as the case for rainfall. Only for 2 years (1982 and 2002) the
 243 AI was higher than 1. During all other years, potential evapotranspiration exceeded rainfall, thus indicating
 244 persistently dry conditions across this catchment.

245 Streamflow data is available at Purapel en Nirivilo between 1979 and 2019 and at Purapel en Sauzal
 246 between 1981-2019. At the annual scale, only 20 and 22, respectively, discontinuous years passed the com-
 247 pleteness test. For the Suspended Sediment Concentration data, the longest period is 1985-2018, but only 15
 248 discontinuous years passed the completeness test. Because most of the annual time-series failed the autocor-
 249 relation and completeness tests, here we report only the seasonal analysis for Purapel en Sauzal station (Fig.
 250 4). Although any of those time-series is monotonic, the sharp decrease in suspended sediment concentrations
 251 is clear for the three wetter seasons (Autumn, Winter and Spring).

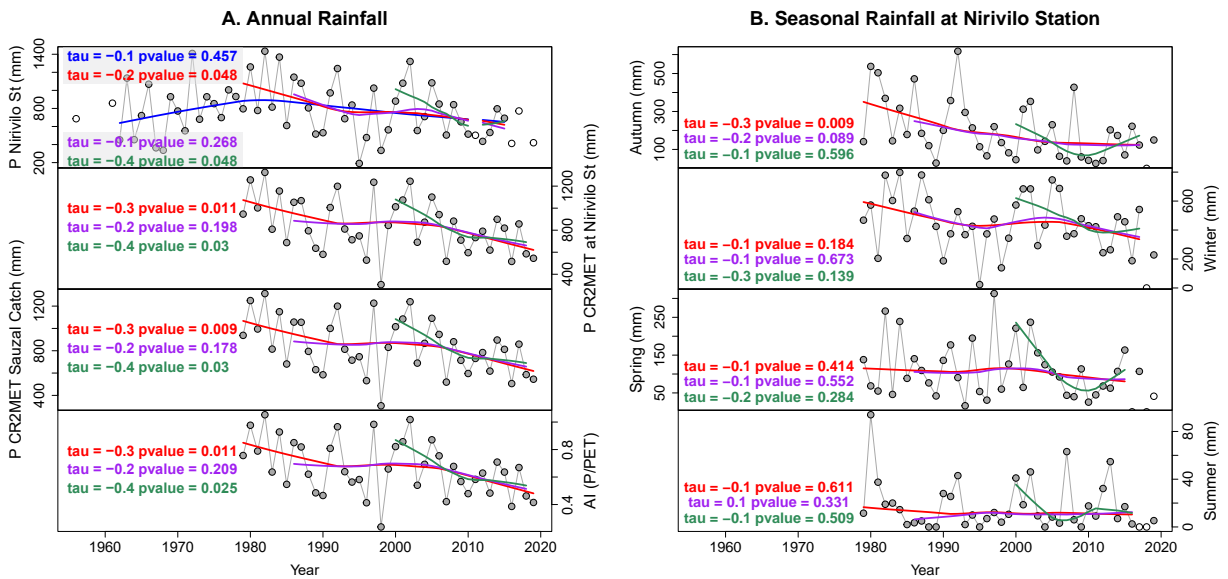


Figure 3: Annual and seasonal rainfall and annual aridity index (AI) at Purapel catchment. Main monotonic trends are tested with Mann-Kendall and LOWESS smoothing for 1962-2015 (blue), 1979-2019 (red), 1986-2018 (purple) and 2000-2018 (green). Unfilled circles are discarded data. A. Annual rainfall and AI time series. B. Seasonal time series for Nirivilo station.

Catchment-wide erosion rates

252 ¹⁰Be denudation rater resulted in 0.024 ± 0.004 mm/yr (table 1), assuming a soil bulk density of 2.6 t/m³.
 253 This rate translates into a sediment yield of 62.4 ± 10.4 tkm⁻²yr⁻¹. This rate integrates over a characteristic
 254 timescale of ~ 25 kyrs. Given the data completeness test, we calculated the decadal catchment-wide erosion
 255 rate using the mean specific sediment discharge for all the records between 1985 and 2018 and a 30% of error
 256 (Pepin et al., 2010). For the Purapel catchment we estimate 46.99 ± 14.09 tkm⁻²yr⁻¹, equal to 0.018 ± 0.005
 257 mm/yr, assuming the same soil bulk density. Both rates do not statistically differ (Fig. 5).
 258

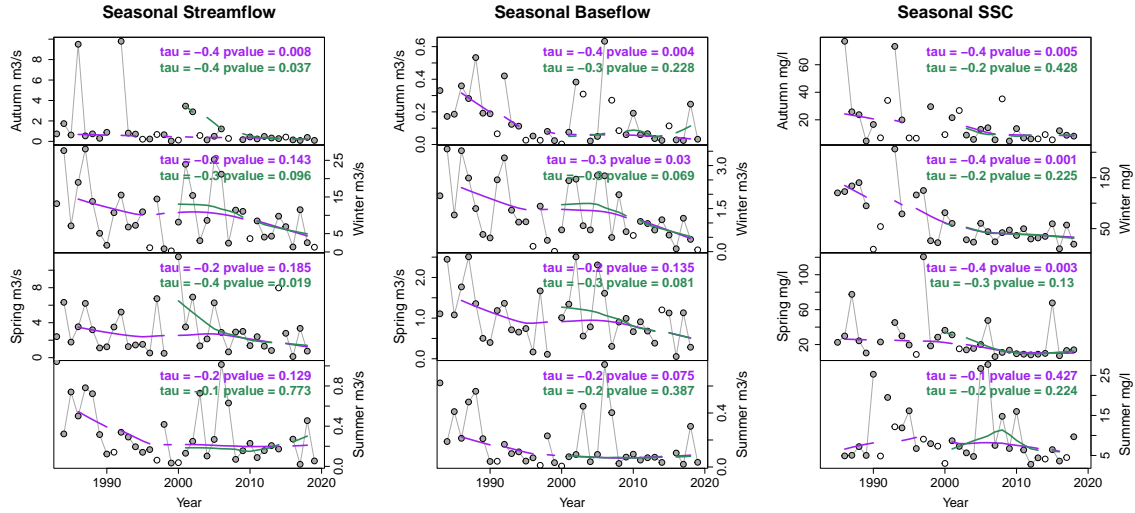


Figure 4: Mean seasonal streamflow, baseflow and suspended sediment concentrations at “Purapel en Sauzal” station. Main monotonic trends are tested with Mann-Kendall and LOWESS smoothing for 1986-2018 (purple) and 2000-2018 (green). Unfilled circles are discarded data. A. Streamflow at Purapel en Sauzal station. C. Suspended sediment concentrations at Purapel en Sauzal station.

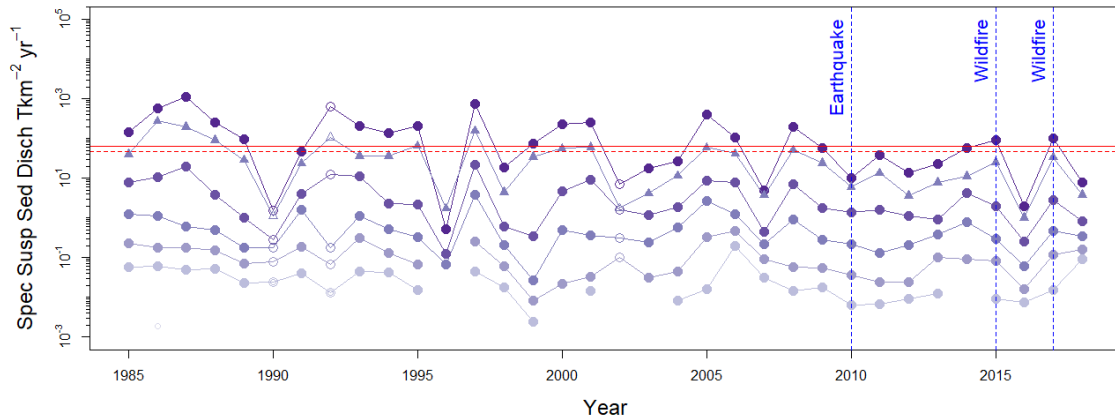


Figure 5: Denudation and specific suspended sediment discharge at Purapel en Sauzal gauge. Distributions of suspended sediment discharge for individual hydrologic years (March to Feb). Purple circles show percentiles (0.05, 0.25, 0.5, 0.75 and 0.95) and purple triangles show the mean. Filled symbols represent years with more than 185 daily data. Catchment erosion/denudation rates are indicated in red. Solid line is the sediment yield equivalent to the ^{10}Be denudation rate, dashed line is the average of all suspended sediment records.

259 Recent land cover changes

260 We developed five land cover maps for the period 1986-2015. The overall classification accuracy ranged
 261 between 83% and 92%. We distinguished between tree plantations, native forests, shrublands and seasonal
 262 grasslands. Seasonal grasslands included bare surfaces, seasonal pasture and sparse vegetation. We also

263 classified seasonal grasslands to separate recently logged areas (clear-cuts) from other poorly vegetated
264 areas.

265 Fig. 6 shows that the upper catchment was covered by a minimum of 1,000 ha of tree plantations and
266 5,500 ha of shrublands in 1955 (Hermosilla-Palma et al., 2021). Between the 1980s and the beginning of
267 21th century, the most prominent change comprised the transition from seasonal grasslands and shrublands
268 into tree plantations. The first two classes covered a minimum of 23,550 ha in 1986 and 13,050 ha on 2005.
269 During the same period, tree plantations expanded from 8,090 to 20,980 ha. Between both wildfires, seasonal
270 grasslands and shrublands together expanded to $\sim 20,300$ ha (Fig. 6).

271 Landscape disturbances

272 The result of our mapped road network is illustrated in Fig. 1. Using this road network on a 5 m resolution
273 LiDAR, we estimate some 18,000 ha of increased sediment connectivity, resulting in $RC > 0$ (Fig. 7). RC
274 values exceeding the 95-percentile (> 3.12) are 1,986 ha. That surface of high RC is mostly located on
275 hilltops: 1,966 ha (i.e. 99%) resulted in upstream contributing area < 1 ha. Particularly these topographic
276 settings exceed an empirical threshold between high and low connectivity for a mountain catchment, i.e.
277 -2.32 (Martini et al., 2022). In the Purapel catchment the area above this threshold increased from 1,120
278 to as much as 6,570 ha simply due to the dense road network. This quantification, however, is done with a
279 digital terrain model of coarser resolution compared to the original study of Martini et al. (2022) (5 m vs
280 0.5 to 2.5 m).

281 Based on our BFAST modeling, we obtained monthly time series of disturbances for 2002-2019 that we
282 sum at the seasonal and annual scale. We achieved an overall accuracy of 77% at an annual scale. For
283 the complete period (Fig. 8A) 13,640 ha of the Purapel catchment (33.7%) experienced one break in the
284 NDVI time series, 16,810 ha (41.5 %) showed two breaks and 5,010 ha (12%) presented three breaks. The
285 undisturbed 12.8% included tree plantation stands that remained unlogged, and seasonal grasslands that
286 remained poorly vegetated. Considering the seasonality (Fig. 8B), the 2015 and 2017 wildfires disturbed the
287 catchment in the summer (dry season). Both wildfires were detected in $\sim 5,000$ and $24,000$ ha, respectively.
288 The disturbances that follow in area ($\sim 2,000$ ha in 2002 and 1,910 ha in 2007) occurred during Autumn,
289 corresponding to the first wet season of the hydrologic year. The largest surface disturbed during a Winter
290 and a Spring were 770 ha each in 2006 and 2009, respectively.

291 Compared to the dNBR classification for 2017 (Tolorza et al., 2022), the BFAST results detected lower
292 burned areas for the 2017 wildfire (33,618 vs 24,299 ha). This difference could be explained by the better
293 capabilities of the dNBR index to detect burned areas, since it is a dedicated method to classify burned
294 surfaces based in the NBR index of a pre- and a post- fire image (Key and Benson, 2006), while the BFAST
295 algorithm was applied here on the NDVI, which is a index more suitable to detect the density of vegetation,
296 and thus more sensitive to clear cuts.

297 Discussion

298 Both ^{10}Be denudation rate and suspended sediment erosion rate are surprisingly similar (Fig. 5). Hence,
299 we argue that the suspended sediment samples capture at least the effects of erosion events recorded on
300 the long-term. Both rates are low for fluvial catchments between 100-1000 km^2 on a global scale (Covault

301 et al., 2013). Yet, those rates are similar than 3 tributaries of the Biobío river draining the eastern CCR,
302 which are between 0.037 ± 0.006 and 0.042 ± 0.008 mm/yr (Carretier et al., 2018). The low ^{10}Be erosion rate
303 agrees with a landscape dominated by slow soil creep with occasional mass wasting triggered by earthquakes.
304 Reported landslides after the 2010 earthquake are only 2 within the catchment area (Serey et al., 2019). Short
305 term erosion does not exceed the long term denudation, as in others highly human-disturbed catchments
306 (Hewawasam et al., 2003; Vanacker et al., 2007). Considering the low number of complete annual records
307 on streamflow and sediment discharge, and the absence of sub-daily or depth-integrated measurements of
308 sediment concentrations, we regard the decadal sediment data as a conservative estimate for recent catchment
309 erosion. This was also reported for suspended sediments from other rivers of the western Andes (Vanacker
310 et al., 2020; Carretier et al., 2018). In addition, suspended sediments do not record the effects of chemical
311 weathering on denudation rates. This process seems to be relevant in the CCR: in the absence of spatially
312 resolved data of regolith thickness, single observations suggest thick saprolite layers (at least) locally (Vázquez
313 et al., 2016; Mohr et al., 2012; Krone et al., 2021). Thus, depending on the magnitude of mass loss due
314 to chemical weathering, total denudation in the short term can be equal or even higher than the long term
315 denudation. Yet, we do not have quantitative estimates of soil production rates to test that hypothesis.

316 The Purapel river catchment has been staging ground for rapid expansion of tree plantations and a
317 number of disturbances during the period of suspended sediment monitoring. This landscape was affected
318 by clear-cuts, two widespread wildfires and one Mw 8.8 earthquake. The expansion of tree plantations was
319 mostly at the expense of poorly vegetated surfaces (Fig. 6). Yet, their management include extensive logging
320 operations – mostly during wet seasons (Fig. 8) – and the construction and maintaining of forestry roads
321 used by heavy machinery. The distribution and density of road network by itself means an increase in
322 structural sediment connectivity (Fig. 7). Higher connectivity facilitates the routing of detached soils, even
323 from hilltops, where soil production rate is slower compared to the mid-slope or toe positions across the
324 CCR (Schaller and Ehlers, 2022). Thus, hilltops soils may be more difficult to recover during human time
325 scales. The increase in sediment connectivity is distributed along all the hillslopes and more than the half of
326 the catchment experienced at least 2 disturbance events between 2002 and 2019. Despite the disturbances,
327 mean and high (p95) annual values of suspended sediment discharge (Fig. 5) and mean suspended sediment
328 concentrations during the wet seasons (Fig. 4) decreased and remained low after the 2017 fire. In contrast,
329 only the lower percentiles of suspended sediment discharge increased after 2017 wildfire. Such behavior
330 corresponds to baseflow conditions. Regardless, we emphasize that the connectivity index here may be a
331 minimum estimate as we used a coarser digital terrain model compared to the original study.

332 If the suspended sediment record is representative of the sediment yields on Purapel river, the disturbance
333 regime contrast with expected responses in sediment mobilization, given observations reported in other
334 landscapes (e.g., Reneau et al., 2007; Brown and Krygier, 1971). Nevertheless, the low values of the AI, i.e.
335 the ratio between annual precipitation and evapotranspiration, indicate increasingly scarce water. A decrease
336 can be also interpreted for the streamflow and the baseflow of the wet seasons, mostly in the Autumn. The
337 sediment detachment and transport may coincide with these negative trends. Sediment mobilization both
338 on hillslopes and streams depends mostly on specific thresholds of rainfall intensity and water discharge,
339 while the unprecedented drought starting in 2010, together with high root water uptake by fast-growing
340 tree plantations result into a reduction in water availability. In this scenario, a lack of minimum rainfall
341 intensity required to trigger runoff and soil erosion on hillslopes (Mohr et al., 2013) and/or an increase in
342 the residence time of sediments stored within the valleys is plausible. As rainfall and direct runoff control

343 sediment fluxes at the catchment scale (Andermann et al., 2012; Tolorza et al., 2014), sediment mobilization
344 under the current hydrological regime may stay low despite landscape disturbances. In fact, after the severe
345 and extended 2017 fire (Fig. 6) and after the M_w 8.8 Maule earthquake (Tolorza et al., 2019), sediment
346 discharge remained low at Purapel river. A recent model in post-fire sediment cascades indicates that, even
347 when post-fire erosion may be severe in source areas, a substantial fraction of the detached sediment load
348 may (intermittently) remain stored within valleys with only moderate delivery to the river network (Murphy
349 et al., 2019). Assuming transport limitation under the current drought conditions, prolonged residence times
350 of sediments may be also expected. Indeed, both tree plantations and the drought reduced the recharge of
351 deep soil water reservoirs (Iroumé et al., 2021; Huber et al., 2010). Also the loss of soils due to erosion
352 may further reduce the water-storage capacity (Ratta and Lal, 1998). The long deficit of water due to the
353 drought and the tree plantations may reduce groundwater storage, which is consistent with the observed
354 negative trend in baseflow. Such sharp reduction in water availability may limit the sediment transport in
355 channels. The increase of the sediment transport only for the lower percentiles supports the notion that
356 sediment transport is largely restricted to baseflow conditions during the study period. Hence, we cannot
357 unambiguously quantify the overall effect of landscape disturbances on sediment fluxes. Sediment fluxes are
358 more efficient during periods of high flows which correspond to wetter conditions (e.g., Mohr et al., 2013).
359 Consequently, the sediment stored in the valleys, highly rich in nutrients and carbon, can be re-suspended
360 during higher discharge events, then causing temporarily delayed off-site problems for several decades to
361 come.

362 The expansion of tree plantations has been proposed as a tool to mitigate soil erosion (CONAF and
363 MINAGRI, 2016). Recently, plantations have been favored as a better solution to mitigate soil erosion
364 compared to native forests for the same Purapel catchment (Pizarro et al., 2020). A direct comparison
365 between native forest and plantations cannot be done for the period 1986-2018, because the major land
366 cover transition was from poorly vegetated surfaces to tree plantations (Fig. 6). Nevertheless, we can
367 discuss if the observed land management is a suitable solution for soil erosion mitigation in the CCR. There
368 is abundant evidence of increased soil erosion in Chilean tree plantations, such as truncated soil profiles in
369 an eucalyptus stand at 36°37'S (Banfield et al., 2018), a fourfold increase in net soil loss under pine stands
370 relative to native forest at Talcamavida (37°7'S) and Nacimiento (37°30'S) (Aburto et al., 2020) or changes
371 in nutrient cycles and increased sedimentation rates in coastal lakes, such as Matanza (33°45'S, Fuentealba
372 et al., 2020), Vichuquén (34°S, Fuentealba et al., 2021), San Pedro (36°51', Cisternas et al., 2001), and
373 Lanalhue (37°S, Alaniz et al., 2021). Based on such strong empirical evidence along CCR and our own
374 results (Fig. 2, 6, 7 and 8), we argue that the observed ongoing forest management of tree plantations
375 promote soil erosion. In addition, soils in tree plantations are depleted in carbon and nutrients (Soto et al.,
376 2019; Banfield et al., 2018), and inhibit lower invertebrate diversity (Cifuentes-Croquevielle et al., 2020)
377 compared to soils under native forest. As a result, C and N stocks are relatively lower in tree plantations up
378 to deep soil compartments (>120 cm) (Crovo et al., 2021). Soil organic matter is a key component for soil
379 formation (Bernhard et al., 2018). Only for that reason, native forests but not exotic tree plantations are a
380 more appropriate land cover to regenerate soils and reverse or, at least, decelerate 200 years of intense soil
381 erosion. Indeed, the protection and conservation of natural vegetation has the strongest effect on soil quality
382 after water erosion (Vanacker et al., 2022), and the few empirical restoration examples of native forest in
383 former Eucalyptus plantations has promising increases for water availability (Lara et al., 2021).

384 Conclusion

385 The Purapel catchment, as other similar catchments along the CCR, denudates slowly. The averaged sus-
386 pended sediment discharge is similarly low, although likely underestimating total denudation. Suspended
387 sediment transport decreases during the wet seasons between 1986 and 2018, which, at a very first glance,
388 conflict with the disturbances observed in vegetation, specially the intense and widespread wildfires. The
389 decrease in several hydroclimatic measures, including baseflow and aridity coincide with this lower suspended
390 sediment loads. We argue that the low range of recent suspended sediment discharge resulted from limita-
391 tions in the detachment and transport of sediments due to the overall observed water scarcity. Or in other
392 words: The drought offsets the effects of the disturbances and the higher connectivity. Without sufficient
393 water, residence times of sediments are long, despite the increased sediment connectivity on hillslopes. The
394 contribution of tree plantations to reduce erosion, if any, seems to be more related to their impact in water
395 availability than directly in soil protection.

396 References

- 397 F. Aburto, E. Cartes, O. Mardones, and R. Rubilar. Hillslope soil erosion and mobility in exotic pine
398 plantations and native deciduous forest in the coastal range of south-central Chile. *Land Degrada-*
399 *tion & Development*, page ldr.3700, 6 2020. ISSN 1085-3278. doi: 10.1002/ldr.3700. URL <https://onlinelibrary.wiley.com/doi/abs/10.1002/ldr.3700>.
- 401 A. J. Alaniz, A. M. Abarzúa, A. Martel-Cea, L. Jarpa, M. Hernández, M. A. Aquino-López, and C. Smith-
402 Ramírez. Linking sedimentological and spatial analysis to assess the impact of the forestry industry on
403 soil loss: The case of Lanalhue Basin, Chile. *Catena*, 207, 12 2021. ISSN 03418162. doi: 10.1016/j.catena.
404 2021.105660.
- 405 C. Álvarez-Garretón, P. A. Mendoza, J. P. Boisier, N. Addor, M. Galleguillos, M. Zambrano-Bigiarini,
406 A. Lara, C. Puelma, G. Cortes, R. Garreaud, J. McPhee, and A. Ayala. The CAMELS-CL dataset:
407 catchment attributes and meteorology for large sample studies – Chile dataset. *Hydrology and Earth*
408 *System Sciences Discussions*, pages 1–40, 2 2018. ISSN 1812-2116. doi: 10.5194/hess-2018-23. URL
409 <https://www.hydrol-earth-syst-sci-discuss.net/hess-2018-23/>.
- 410 C. Andermann, A. Crave, R. Gloaguen, P. Davy, and S. Bonnet. Connecting source and transport: Suspended
411 sediments in the Nepal Himalayas. *Earth and Planetary Science Letters*, 351-352:158–170, 2012. ISSN
412 0012821X. doi: 10.1016/j.epsl.2012.06.059. URL <http://dx.doi.org/10.1016/j.epsl.2012.06.059>.
- 413 J. J. Armesto, D. Manuschevich, A. Mora, C. Smith-Ramirez, R. Rozzi, A. M. Abarzúa, and P. a. Marquet.
414 From the Holocene to the Anthropocene: A historical framework for land cover change in southwestern
415 South America in the past 15,000 years. *Land Use Policy*, 27(2):148–160, 2010. ISSN 02648377. doi:
416 10.1016/j.landusepol.2009.07.006. URL <http://dx.doi.org/10.1016/j.landusepol.2009.07.006>.
- 417 C. C. Banfield, A. C. Braun, R. Barra, A. Castillo, and J. Vogt. Erosion proxies in an exotic tree
418 plantation question the appropriate land use in Central Chile. *CATENA*, 161:77–84, 2 2018. ISSN
419 03418162. doi: 10.1016/j.catena.2017.10.017. URL <http://linkinghub.elsevier.com/retrieve/pii/S0341816217303399>.

- 421 S. Barros. Evolución de las plantaciones forestales en Chile. Forestación y reforestación. *Ciencia e In-*
422 *vestigación Forestal*, 24(3):89–115, 2018. URL [https://bibliotecadigital.infor.cl/handle/20.500.](https://bibliotecadigital.infor.cl/handle/20.500.12220/28235)
423 [12220/28235](https://bibliotecadigital.infor.cl/handle/20.500.12220/28235).
- 424 N. Bernhard, L.-M. Moskwa, K. Schmidt, R. A. Oeser, F. Aburto, M. Y. Bader, K. Baumann, F. von
425 Blanckenburg, J. Boy, L. van den Brink, E. Brucker, B. Büdel, R. Canessa, M. A. Dippold, T. A. Ehlers,
426 J. P. Fuentes, R. Godoy, P. Jung, U. Karsten, M. Köster, Y. Kuzyakov, P. Leinweber, H. Neidhardt,
427 F. Matus, C. W. Mueller, Y. Oelmann, R. Oses, P. Osses, L. Paulino, E. Samolov, M. Schaller,
428 M. Schmid, S. Spielvogel, M. Spohn, S. Stock, N. Stroncik, K. Tielbörger, K. Übernicker, T. Scholten,
429 O. Seguel, D. Wagner, and P. Kühn. Pedogenic and microbial interrelations to regional climate and
430 local topography: New insights from a climate gradient (arid to humid) along the Coastal Cordillera
431 of Chile. *CATENA*, 170:335–355, 11 2018. ISSN 03418162. doi: 10.1016/j.catena.2018.06.018. URL
432 <https://doi.org/10.1016/j.catena.2018.06.018>[https://linkinghub.elsevier.com/retrieve/](https://linkinghub.elsevier.com/retrieve/pii/S0341816218302509)
433 [pii/S0341816218302509](https://www.researchgate.net/publication/268272012_Tools_to_aid_post-wildfire_assessment_and_erosion-mitigation_treatment_decisions)[https://www.researchgate.net/publication/268272012_Tools_to_aid_](https://www.researchgate.net/publication/268272012_Tools_to_aid_post-wildfire_assessment_and_erosion-mitigation_treatment_decisions)
434 [post-wildfire_assessment_and_erosion-mitigation_treatment_decisions](https://www.researchgate.net/publication/268272012_Tools_to_aid_post-wildfire_assessment_and_erosion-mitigation_treatment_decisions).
- 435 V. Bianchi-Gundian. *Erosión. Cáncer del suelo*. Imprenta Universitaria, Santiago de Chile, 1947.
- 436 K. D. Bladon, M. B. Emelko, U. Silins, and M. Stone. Wildfire and the Future of Water Supply. *Environ-*
437 *mental Science & Technology*, 48(16):8936–8943, 8 2014. ISSN 0013-936X. doi: 10.1021/es500130g. URL
438 <https://pubs.acs.org/doi/10.1021/es500130g>.
- 439 J. Boardman, K. Vandaele, R. Evans, and I. D. Foster. Off-site impacts of soil erosion and runoff: Why
440 connectivity is more important than erosion rates. *Soil Use and Management*, 35(2):245–256, 6 2019. ISSN
441 14752743. doi: 10.1111/sum.12496.
- 442 J. P. Boisier, C. Alvarez-Garretón, J. Cepeda, A. Osses, N. Vásquez, and R. Rondanelli. CR2MET: A high-
443 resolution precipitation and temperature dataset for hydroclimatic research in Chile. In *EGU General*
444 *Assembly Conference Abstracts*, EGU General Assembly Conference Abstracts, page 19739, 4 2018a. URL
445 <https://meetingorganizer.copernicus.org/EGU2018/EGU2018-19739.pdf>.
- 446 J. P. Boisier, C. Alvarez-Garretón, R. R. Cordero, A. Damiani, L. Gallardo, R. D. Garreaud, F. Lambert,
447 C. Ramallo, M. Rojas, and R. Rondanelli. Anthropogenic drying in central-southern Chile evidenced
448 by long-term observations and climate model simulations. *Elementa*, 6, 2018b. ISSN 23251026. doi:
449 10.1525/elementa.328.
- 450 C. A. Bonilla and O. I. Johnson. Soil erodibility mapping and its correlation with soil properties in Central
451 Chile. *Geoderma*, 189-190:116–123, 11 2012. ISSN 00167061. doi: 10.1016/j.geoderma.2012.05.005. URL
452 <https://linkinghub.elsevier.com/retrieve/pii/S0016706112001966>.
- 453 P. Borrelli, D. A. Robinson, P. Panagos, E. Lugato, J. E. Yang, C. Alewell, D. Wuepper, L. Montanarella, and
454 C. Ballabio. Land use and climate change impacts on global soil erosion by water (2015-2070). *Proceedings*
455 *of the National Academy of Sciences of the United States of America*, 117(36):21994–22001, 2020. ISSN
456 10916490. doi: 10.1073/pnas.2001403117.
- 457 D. M. J. S. Bowman, A. Moreira-Muñoz, C. A. Kolden, R. O. Chávez, A. A. Muñoz, F. Salinas, A. González-
458 Reyes, R. Rocco, F. de la Barrera, G. J. Williamson, N. Borchers, L. A. Cifuentes, J. T. Abatzoglou, and

459 F. H. Johnston. Human–environmental drivers and impacts of the globally extreme 2017 Chilean fires.
460 *Ambio*, 48(4):350–362, 4 2019. ISSN 0044-7447. doi: 10.1007/s13280-018-1084-1.

461 G. W. Brown and J. T. Krygier. Clear-Cut Logging and Sediment Production in the Oregon Coast Range.
462 *Water Resources Research*, 7(5):1189–1198, 1971. ISSN 19447973. doi: 10.1029/WR007i005p01189.

463 J. Cabezas and F. E. Fassnacht. Reconstructing the Vegetation Disturbance History of a Biodiversity Hotspot
464 in Central Chile Using Landsat, Bfast and Landtrendr. In *IGARSS 2018 - 2018 IEEE International*
465 *Geoscience and Remote Sensing Symposium*, pages 7636–7639. IEEE, 7 2018. ISBN 978-1-5386-7150-4.
466 doi: 10.1109/IGARSS.2018.8518863.

467 S. Carretier, V. Tolorza, V. Regard, G. Aguilar, M. Bermúdez, J. Martinod, J.-L. Guyot, G. Hérail,
468 and R. Riquelme. Review of erosion dynamics along the major N-S climatic gradient in Chile and
469 perspectives. *Geomorphology*, 300:45–68, 1 2018. ISSN 0169555X. doi: 10.1016/j.geomorph.2017.
470 10.016. URL <https://www.sciencedirect.com/science/article/pii/S0169555X17304506>[https://](https://linkinghub.elsevier.com/retrieve/pii/S0169555X17304506)
471 linkinghub.elsevier.com/retrieve/pii/S0169555X17304506.

472 M. Cavalli, S. Trevisani, F. Comiti, and L. Marchi. Geomorphometric assessment of spatial sediment
473 connectivity in small Alpine catchments. *Geomorphology*, 188:31–41, 2013. ISSN 0169555X. doi:
474 10.1016/j.geomorph.2012.05.007. URL <http://dx.doi.org/10.1016/j.geomorph.2012.05.007>.

475 Chilean Law 19.300. Decreto 40. Reglamento del Sistema de Evaluación de Impacto Ambiental, 2013. URL
476 <http://bcn.cl/2f8a8>.

477 E. Chuvieco. *Teledeteccion Ambiental: la observacion de la tierra desde el espacio. 3a edicion*. Ariel Ciencia,
478 Barcelona, 2008. ISBN 978-84-344-8072-8.

479 C. Cifuentes-Croquevielle, D. E. Stanton, and J. J. Armesto. Soil invertebrate diversity loss and func-
480 tional changes in temperate forest soils replaced by exotic pine plantations. *Scientific Reports*, 10(1):
481 7762, 12 2020. ISSN 2045-2322. doi: 10.1038/s41598-020-64453-y. URL <http://dx.doi.org/10.1038/>
482 [s41598-020-64453-y](http://www.nature.com/articles/s41598-020-64453-y)<http://www.nature.com/articles/s41598-020-64453-y>.

483 CIREN. Cuenca Río Purapel (Estados erosivos actuales), 2021. URL [http://erosionmaule.ciren.cl/](http://erosionmaule.ciren.cl/documents/348)
484 [documents/348](http://erosionmaule.ciren.cl/documents/348).

485 M. Cisternas, A. Araneda, P. Martinez, and S. Perez. Effects of historical land use on sediment yield
486 from a lacustrine watershed in central Chile. *Earth Surface Processes and Landforms*, 26(1):63–76, 1
487 2001. ISSN 0197-9337. doi: 10.1002/1096-9837(200101)26:1<63::AID-ESP157>3.0.CO;2-J. URL [https://onlinelibrary.wiley.com/doi/10.1002/1096-9837\(200101\)26:1<63::AID-ESP157>3.0.CO;2-J](https://onlinelibrary.wiley.com/doi/10.1002/1096-9837(200101)26:1<63::AID-ESP157>3.0.CO;2-J).

488 [https://onlinelibrary.wiley.com/doi/10.1002/1096-9837\(200101\)26:1<63::AID-ESP157>3.0.CO;2-J](https://onlinelibrary.wiley.com/doi/10.1002/1096-9837(200101)26:1<63::AID-ESP157>3.0.CO;2-J).

489 W. S. Cleveland. LOWESS: A Program for Smoothing Scatterplots by Robust Locally Weighted Regression.
490 *The American Statistician*, 35(1):54, 2 1981. ISSN 00031305. doi: 10.2307/2683591. URL [https://www.](https://www.jstor.org/stable/2683591?origin=crossref)
491 [jstor.org/stable/2683591?origin=crossref](https://www.jstor.org/stable/2683591?origin=crossref).

492 CONAF and MINAGRI. Decreto Ley 701 de 1974, Cuarenta años de incentivos a la forestación (1975-2015),
493 2016. URL <https://biblioteca.digital.gob.cl/handle/123456789/2334>.

- 494 L. Cortés, H. J. Hernández, and P. Silva. Historic Land Cover Change assesment of Chilean
495 Mediterranean Coast: Did forest plantations really caused fragmentation? *ISPRS Annals*
496 *of the Photogrammetry, Remote Sensing and Spatial Information Sciences*, V-3-2022:383–388, 5
497 2022. ISSN 2194-9050. doi: 10.5194/isprs-annals-V-3-2022-383-2022. URL [https://www.
498 isprs-ann-photogramm-remote-sens-spatial-inf-sci.net/V-3-2022/383/2022/](https://www.isprs-ann-photogramm-remote-sens-spatial-inf-sci.net/V-3-2022/383/2022/).
- 499 J. A. Covault, W. H. Craddock, B. W. Romans, A. Fildani, and M. Gosai. Spatial and Temporal Variations in
500 Landscape Evolution: Historic and Longer-Term Sediment Flux through Global Catchments. *The Journal*
501 *of Geology*, 121(1):35–56, 1 2013. ISSN 00221376. doi: 10.1086/668680. URL [http://www.jstor.org/
502 stable/info/10.1086/668680](http://www.jstor.org/stable/info/10.1086/668680).
- 503 O. Crovo, F. Aburto, M. F. Albornoz, and R. Southard. Soil type modulates the response of C, N, P
504 stocks and stoichiometry after native forest substitution by exotic plantations. *CATENA*, 197:104997, 2
505 2021. ISSN 03418162. doi: 10.1016/j.catena.2020.104997. URL [https://linkinghub.elsevier.com/
506 retrieve/pii/S0341816220305476](https://linkinghub.elsevier.com/retrieve/pii/S0341816220305476).
- 507 D. A. DellaSala. “Real” vs. “Fake” Forests: Why Tree Plantations Are Not Forests. In *Encyclo-*
508 *pedia of the World’s Biomes*, volume 3-5, pages 47–55. Elsevier, 6 2020. ISBN 9780128160978.
509 doi: 10.1016/B978-0-12-409548-9.11684-7. URL [https://linkinghub.elsevier.com/retrieve/pii/
510 B9780124095489116847](https://linkinghub.elsevier.com/retrieve/pii/B9780124095489116847).
- 511 E. C. Ellis and N. Ramankutty. Putting people in the map: anthropogenic biomes of the world. *Frontiers*
512 *in Ecology and the Environment*, 6(8):439–447, 10 2008. ISSN 1540-9295. doi: 10.1890/070062. URL
513 <http://doi.wiley.com/10.1890/070062>.
- 514 S. Foga, P. L. Scaramuzza, S. Guo, Z. Zhu, R. D. Dilley, T. Beckmann, G. L. Schmidt, J. L. Dwyer,
515 M. Joseph Hughes, and B. Laue. Cloud detection algorithm comparison and validation for operational
516 Landsat data products. *Remote Sensing of Environment*, 194:379–390, 6 2017. ISSN 00344257. doi:
517 10.1016/j.rse.2017.03.026.
- 518 M. Fuentealba, C. Latorre, M. Frugone-Álvarez, P. Sarricolea, S. Giralt, M. Contreras-Lopez, R. Prego,
519 P. Bernárdez, and B. Valero-Garcés. A combined approach to establishing the timing and magnitude of
520 anthropogenic nutrient alteration in a mediterranean coastal lake- watershed system. *Scientific Reports*,
521 10(1):5864, 12 2020. ISSN 2045-2322. doi: 10.1038/s41598-020-62627-2. URL [http://www.nature.com/
522 articles/s41598-020-62627-2](http://www.nature.com/articles/s41598-020-62627-2).
- 523 M. Fuentealba, C. Latorre, M. Frugone-Álvarez, P. Sarricolea, C. Godoy-Aguirre, J. Armesto, L. A. Villacís,
524 M. Laura Carrevedo, O. Meseguer-Ruiz, and B. Valero-Garcés. Crossing a critical threshold: Accelerated
525 and widespread land use changes drive recent carbon and nitrogen dynamics in Vichuquén Lake (35°S) in
526 central Chile. *Science of the Total Environment*, 791, 10 2021. ISSN 18791026. doi: 10.1016/j.scitotenv.
527 2021.148209.
- 528 E. J. Gabet, S. M. Mudd, R. W. Wood, S. W. D. Grieve, S. A. Binnie, and T. J. Dunai. Hilltop Curvature
529 Increases With the Square Root of Erosion Rate. *Journal of Geophysical Research: Earth Surface*, 126(5):
530 1–16, 2021. ISSN 2169-9003. doi: 10.1029/2020jf005858.

- 531 M. Galleguillos, F. Gimeno, C. Puelma, M. Zambrano-Bigiarini, A. Lara, and M. Rojas. Disentangling
532 the effect of future land use strategies and climate change on streamflow in a Mediterranean catchment
533 dominated by tree plantations. *Journal of Hydrology*, 595(February), 2021. ISSN 00221694. doi: 10.1016/
534 j.jhydrol.2021.126047.
- 535 R. D. Garreaud, J. P. Boisier, R. Rondanelli, A. Montecinos, H. H. Sepúlveda, and D. Veloso-Aguila.
536 The Central Chile Mega Drought (2010–2018): A climate dynamics perspective. *International Jour-
537 nal of Climatology*, 40(1):421–439, 1 2020. ISSN 0899-8418. doi: 10.1002/joc.6219. URL <https://onlinelibrary.wiley.com/doi/10.1002/joc.6219>.
- 538
- 539 V. Gerding. Manejo de las plantaciones de *Pinus radiata* D. Don en Chile. *Bosque*, 12(2):3–10, 1991.
- 540 F. Gimeno, M. Galleguillos, D. Manushevich, and M. Zambrano-Bigiarini. A coupled modeling approach
541 to assess the effect of forest policies in water provision: A biophysical evaluation of a drought-prone rural
542 catchment in south-central Chile. *Science of The Total Environment*, 830:154608, 7 2022. ISSN 00489697.
543 doi: 10.1016/j.scitotenv.2022.154608.
- 544 S. Gómez-González, S. Paula, L. A. Cavieres, and J. G. Pausas. Postfire responses of the woody flora of
545 Central Chile: Insights from a germination experiment. *PLoS ONE*, 12(7):1–12, 2017. ISSN 19326203.
546 doi: 10.1371/journal.pone.0180661.
- 547 S. Gómez-González, F. Ojeda, and P. M. Fernandes. Portugal and Chile: Longing for sustainable
548 forestry while rising from the ashes. *Environmental Science & Policy*, 81:104–107, 3 2018. ISSN
549 14629011. doi: 10.1016/j.envsci.2017.11.006. URL [https://linkinghub.elsevier.com/retrieve/pii/
550 S1462901117307694](https://linkinghub.elsevier.com/retrieve/pii/S1462901117307694).
- 551 D. E. Granger and M. Schaller. Cosmogenic Nuclides and Erosion at the Watershed Scale. *Elements*,
552 10(5):369–373, 10 2014. ISSN 1811-5209. doi: 10.2113/gselements.10.5.369. URL [https://pubs.
553 geoscienceworld.org/elements/article/10/5/369-373/137626](https://pubs.geoscienceworld.org/elements/article/10/5/369-373/137626).
- 554 M. C. Hansen, P. V. Potapov, R. Moore, M. Hancher, S. A. Turubanova, A. Tyukavina, D. Thau, S. V.
555 Stehman, S. J. Goetz, T. R. Loveland, A. Kommareddy, A. Egorov, L. Chini, C. O. Justice, and J. R. G.
556 Townshend. High-Resolution Global Maps of 21st-Century Forest Cover Change. *Science*, 342(6160):
557 850–853, 11 2013. ISSN 0036-8075. doi: 10.1126/science.1244693. URL [http://www.sciencemag.org/
558 cgi/doi/10.1126/science.1244693](http://www.sciencemag.org/cgi/doi/10.1126/science.1244693).
- 559 R. Heilmayr, C. Echeverría, R. Fuentes, and E. F. Lambin. A plantation-dominated forest transition in
560 Chile. *Applied Geography*, 75:71–82, 2016. ISSN 01436228. doi: 10.1016/j.apgeog.2016.07.014. URL
561 <http://dx.doi.org/10.1016/j.apgeog.2016.07.014>.
- 562 D. R. Helsel, R. M. Hirsch, K. R. Ryberg, S. A. Archfield, and E. J. Gilroy. Statistical methods in water
563 resources. Technical report, USGS, Reston, VA, 2020. URL [http://pubs.er.usgs.gov/publication/
564 tm4A3](http://pubs.er.usgs.gov/publication/tm4A3).
- 565 K. Hermosilla-Palma, P. Pliscoff, and M. Folchi. Sixty years of land-use and land-cover change dynamics in
566 a global biodiversity hotspot under threat from global change. *Journal of Land Use Science*, 16(5-6):467–
567 478, 11 2021. ISSN 1747-423X. doi: 10.1080/1747423X.2021.2011970. URL [https://www.tandfonline.
568 com/doi/full/10.1080/1747423X.2021.2011970](https://www.tandfonline.com/doi/full/10.1080/1747423X.2021.2011970).

- 569 T. Hewawasam, F. von Blanckenburg, M. Schaller, and P. Kubik. Increase of human over natural erosion
570 rates in tropical highlands constrained by cosmogenic nuclides. *Geology*, 31(7):597–600, 2003. ISSN
571 00917613. doi: 10.1130/0091-7613(2003)031<0597:IOHONE>2.0.CO;2. URL <http://geology.gsapubs.org/content/31/7/597.abstract>.
- 573 A. Huber, A. Iroumé, C. Mohr, and C. Frêne. Effect of *Pinus radiata* and *Eucalyptus globulus* plantations on
574 water resource in the Coastal Range of Biobio region, Chile. *Bosque (Valdivia)*, 31(3):219–230, 2010. ISSN
575 0717-9200. doi: 10.4067/S0717-92002010000300006. URL http://www.scielo.cl/scielo.php?script=sci_arttext&pid=S0717-92002010000300006&lng=en&nrm=iso&tlng=en.
- 577 F. Imaizumi, R. C. Sidle, and R. Kamei. Effects of forest harvesting on the occurrence of landslides and
578 debris flows in steep terrain of central Japan. *Earth Surface Processes and Landforms*, 33(6):827–840, 5
579 2008. ISSN 01979337. doi: 10.1002/esp.1574. URL <http://www3.interscience.wiley.com/journal/121517813/abstracthttp://doi.wiley.com/10.1002/esp.1574>.
- 581 INFOR. Informe Técnico 165: *Eucalyptus nitens* en Chile: primera monografía. Technical report, INFOR,
582 Valdivia, 2004. URL <https://bibliotecadigital.infor.cl/handle/20.500.12220/7741?show=full>.
- 583 IPCC. Regional Fact Sheet – Central and South America in: Sixth Assessment Report. Working Group I –
584 The Physical Science Basis. *Ippc*, page 2, 2021. URL <https://www.ipcc.ch/assessment-report/ar6/>.
- 585 IREN. Evaluación de la erosión Cordillera de la Costa entre Valparaíso y Cautín. Technical report, Instituto
586 de Investigación de Recursos Naturales, Instituto de Investigación de Recursos Naturales, Santiago, Chile,
587 1965. URL <http://bibliotecadigital.ciren.cl/handle/123456789/14283>.
- 588 A. Iroumé, O. Mayen, and A. Huber. Runoff and peak flow responses to timber harvest and forest age in
589 southern Chile. *Hydrological Processes*, 20(1):37–50, 2006. ISSN 08856087. doi: 10.1002/hyp.5897.
- 590 A. Iroumé, J. Jones, and J. C. Bathurst. Forest operations, tree species composition and decline in rainfall
591 explain runoff changes in the Nacimiento experimental catchments, south central Chile. *Hydrological*
592 *Processes*, 35(6):1–21, 2021. ISSN 0885-6087. doi: 10.1002/hyp.14257.
- 593 C. H. Key and N. C. Benson. Landscape Assessment (LA) sampling and analysis methods. In *Lutes, Duncan*
594 *C.; Keane, Robert E.; Caratti, John F.; Key, Carl H.; Benson, Nathan C.; Sutherland, Steve; Gangi, Larry*
595 *J. FIREMON: Fire effects monitoring and inventory system. Gen. Tech. Rep. RMRS-GTR-164-CD*, pages
596 LA1–LA51. US Department of Agriculture, Forest Service, Rocky Mountain Research Station, 2006. URL
597 <https://www.fs.usda.gov/treearch/pubs/24066>.
- 598 J. W. Kirchner, R. C. Finkel, C. S. Riebe, D. E. Granger, J. L. Clayton, J. G. King, and W. F. Megahan.
599 Mountain erosion over 10 yr, 10 k.y., and 10 m.y. time scales. *Geology*, 29(7):591, 2001. ISSN 0091-7613. doi:
600 10.1130/0091-7613(2001)029<0591:MEOYKY>2.0.CO;2. URL <http://geology.gsapubs.org/content/29/7/591.abstracthttps://pubs.geoscienceworld.org/geology/article/29/7/591-594/188782>.
- 602 L. V. Krone, F. J. Hampl, C. Schwerdhelm, C. Bryce, L. Ganzert, A. Kitte, K. Übernickel, A. Dielforder,
603 S. Aldaz, R. Osés-Pedraza, J. P. H. Perez, P. Sanchez-Alfaro, D. Wagner, U. Weckmann, and F. von
604 Blanckenburg. Deep weathering in the semi-arid Coastal Cordillera, Chile. *Scientific Reports*, 11(1), 12
605 2021. ISSN 20452322. doi: 10.1038/s41598-021-90267-7.

- 606 A. Ladson, R. Brown, B. Neal, and R. Nathan. A standard approach to baseflow separation using the Lyne
607 and Hollick filter. *Australian Journal of Water Resources*, 17(1), 2013. ISSN 13241583. doi: 10.7158/
608 W12-028.2013.17.1. URL [http://www.engineersmedia.com.au/journals/ajwr/2013/17_1/W12_028.](http://www.engineersmedia.com.au/journals/ajwr/2013/17_1/W12_028.html)
609 [html](http://www.engineersmedia.com.au/journals/ajwr/2013/17_1/W12_028.html).
- 610 A. Lara, J. Jones, C. Little, and N. Vergara. Streamflow response to native forest restoration in former
611 Eucalyptus plantations in south central Chile. *Hydrological Processes*, 35(8), 8 2021. ISSN 10991085. doi:
612 10.1002/hyp.14270.
- 613 A. Malmer and H. Grip. Soil disturbance and loss of infiltrability caused by mechanized and manual ex-
614 traction of tropical rainforest in Sabah, Malaysia. *Forest Ecology and Management*, 38(1-2):1–12, 12
615 1990. ISSN 03781127. doi: 10.1016/0378-1127(90)90081-L. URL [http://linkinghub.elsevier.com/](http://linkinghub.elsevier.com/retrieve/pii/037811279090081L)
616 [retrieve/pii/037811279090081L](http://linkinghub.elsevier.com/retrieve/pii/037811279090081L).
- 617 D. Manuschevich. Land use as a socio-ecological system: Developing a transdisciplinary approach to studies
618 of land use change in South-Central Chile. In *Ecological Economic and Socio Ecological Strategies for*
619 *Forest Conservation: A Transdisciplinary Approach Focused on Chile and Brazil*, pages 79–97. Springer
620 International Publishing, 1 2020. ISBN 9783030353797. doi: 10.1007/978-3-030-35379-7{_}5.
- 621 L. Martini, M. Cavalli, and L. Picco. Predicting sediment connectivity in a mountain basin: A quantitative
622 analysis of the index of connectivity. *Earth Surface Processes and Landforms*, 5 2022. ISSN 10969837.
623 doi: 10.1002/esp.5331.
- 624 M. A. Martins, A. I. Machado, D. Serpa, S. A. Prats, S. R. Faria, M. E. Varela, O. González-Pelayo, and
625 J. J. Keizer. Runoff and inter-rill erosion in a Maritime Pine and a Eucalypt plantation following wildfire
626 and terracing in north-central Portugal. *Journal of Hydrology and Hydromechanics*, 61(4):261–268, 12
627 2013. ISSN 0042-790X. doi: 10.2478/johh-2013-0033. URL [https://content.sciendo.com/doi/10.](https://content.sciendo.com/doi/10.2478/johh-2013-0033)
628 [2478/johh-2013-0033](https://content.sciendo.com/doi/10.2478/johh-2013-0033).
- 629 C. Mohr. *Hydrological and erosion responses to man-made and natural disturbances – Insights from forested*
630 *catchments in South-central Chile*. PhD thesis, University of Potsdam, 2013. URL [https://publishup.](https://publishup.uni-potsdam.de/opus4-ubp/frontdoor/deliver/index/docId/6782/file/mohr_diss.pdf)
631 [uni-potsdam.de/opus4-ubp/frontdoor/deliver/index/docId/6782/file/mohr_diss.pdf](https://publishup.uni-potsdam.de/opus4-ubp/frontdoor/deliver/index/docId/6782/file/mohr_diss.pdf).
- 632 C. H. Mohr, D. R. Montgomery, A. Huber, A. Bronstert, and A. Iroumé. Streamflow response in small
633 upland catchments in the Chilean coastal range to the Mw 8.8 Maule earthquake on 27 February 2010.
634 *Journal of Geophysical Research*, 117(F2):F02032, 6 2012. ISSN 0148-0227. doi: 10.1029/2011JF002138.
635 URL <http://doi.wiley.com/10.1029/2011JF002138>.
- 636 C. H. Mohr, R. Coppus, A. Iroumé, A. Huber, and A. Bronstert. Runoff generation and soil erosion processes
637 after clear cutting. *Journal of Geophysical Research: Earth Surface*, 118(2):814–831, 2013. ISSN 21699003.
638 doi: 10.1002/jgrf.20047. URL <http://doi.wiley.com/10.1002/jgrf.20047>.
- 639 C. H. Mohr, A. Zimmermann, O. Korup, A. Iroumé, T. Francke, and A. Bronstert. Seasonal logging, process
640 response, and geomorphic work. *Earth Surface Dynamics*, 2(1):117–125, 3 2014. ISSN 2196-632X. doi:
641 10.5194/esurf-2-117-2014. URL <http://www.earth-surf-dynam.net/2/117/2014/>.

- 642 D. R. Montgomery, K. M. Schmidt, H. M. Greenberg, and W. E. Dietrich. Forest clearing and regional
643 landsliding. *Geology*, 28(4):311–314, 2000. ISSN 00917613. doi: 10.1130/0091-7613(2000)28(311:FCARL)
644 2.0.CO;2.
- 645 J. A. Moody and D. A. Martin. Synthesis of sediment yields after wildland fire in different rainfall regimes
646 in the western United States. *International Journal of Wildland Fire*, 18(1):96, 2009. ISSN 1049-8001.
647 doi: 10.1071/WF07162. URL <http://www.publish.csiro.au/?paper=WF07162>.
- 648 B. P. Murphy, J. A. Czuba, and P. Belmont. Post-wildfire sediment cascades: A modeling framework linking
649 debris flow generation and network-scale sediment routing. *Earth Surface Processes and Landforms*, 44
650 (11):2126–2140, 9 2019. ISSN 0197-9337. doi: 10.1002/esp.4635. URL <https://onlinelibrary.wiley.com/doi/10.1002/esp.4635>.
- 652 E. Pepin, S. Carretier, J. L. Guyot, and F. Escobar. Specific suspended sediment yields of the Andean rivers
653 of Chile and their relationship to climate, slope and vegetation. *Hydrological Sciences Journal*, 55(7):1190–
654 1205, 10 2010. ISSN 0262-6667. doi: 10.1080/02626667.2010.512868. URL <http://www.tandfonline.com/doi/abs/10.1080/02626667.2010.512868>.
- 656 R. Pizarro, P. García-Chevesich, J. Pino, A. Ibáñez, F. Pérez, J. P. Flores, J. O. Sharp, B. Ingram,
657 R. Mendoza, D. G. Neary, C. Sangüesa, and C. Vallejos. Stabilization of stage–discharge curves
658 following the establishment of forest plantations: Implications for sediment production. *River Re-*
659 *search and Applications*, 36(9):1828–1837, 11 2020. ISSN 1535-1459. doi: 10.1002/rra.3718. URL
660 <https://onlinelibrary.wiley.com/doi/10.1002/rra.3718>.
- 661 R. Ratta and R. Lal. *Soil quality and soil erosion*. CRC press, 1998. ISBN 1351415735, 9781351415736.
- 662 S. L. Reneau, D. Katzman, G. A. Kuyumjian, A. Lavine, and D. V. Malmon. Sediment delivery after a
663 wildfire. *Geology*, 35(2):151–154, 2007. ISSN 00917613. doi: 10.1130/G23288A.1.
- 664 J. J. Roering, J. T. Perron, and J. W. Kirchner. Functional relationships between denudation and hillslope
665 form and relief. *Earth and Planetary Science Letters*, 264(1-2):245–258, 2007. ISSN 0012821X. doi:
666 10.1016/j.epsl.2007.09.035.
- 667 M. Schaller and T. A. Ehlers. Comparison of soil production, chemical weathering, and physical erosion rates
668 along a climate and ecological gradient (Chile) to global observations. *Earth Surface Dynamics*, 10(1):
669 131–150, 2 2022. ISSN 2196-632X. doi: 10.5194/esurf-10-131-2022. URL <https://esurf.copernicus.org/articles/10/131/2022/>.
- 671 P. Schuller, D. E. Walling, A. Iroumé, C. Quilodrán, A. Castillo, and A. Navas. Using ^{137}Cs and ^{210}Pb and
672 other sediment source fingerprints to document suspended sediment sources in small forested catchments
673 in south-central Chile. *Journal of Environmental Radioactivity*, 124:147–159, 2013. ISSN 0265931X. doi:
674 10.1016/j.jenvrad.2013.05.002. URL <http://dx.doi.org/10.1016/j.jenvrad.2013.05.002>.
- 675 P. Schuller, D. E. Walling, A. Iroumé, C. Quilodrán, and A. Castillo. Quantifying the temporal vari-
676 ation of the contribution of fine sediment sources to sediment yields from Chilean forested catch-
677 ments during harvesting operations. *Bosque (Valdivia)*, 42(2):231–244, 2021. ISSN 0717-9200. doi:
678 10.4067/s0717-92002021000200231.

- 679 A. Serey, L. Piñero-Feliciangeli, S. A. Sepúlveda, F. Poblete, D. N. Petley, and W. Murphy. Landslides
680 induced by the 2010 Chile megathrust earthquake: a comprehensive inventory and correlations with
681 geological and seismic factors. *Landslides*, 3 2019. ISSN 1612-510X. doi: 10.1007/s10346-019-01150-6.
682 URL <http://link.springer.com/10.1007/s10346-019-01150-6>.
- 683 R. C. Sidle and A. D. Ziegler. The dilemma of mountain roads, 7 2012. ISSN 17520894.
- 684 W. Solar. Manual de terreno y centros de filtrado. Dirección General de Aguas, 1999. URL <https://snia.mop.gob.cl/sad/SED4939.pdf>.
- 686 L. Soto, M. Galleguillos, O. Seguel, B. Sotomayor, and A. Lara. Assessment of soil physical properties'
687 statuses under different land covers within a landscape dominated by exotic industrial tree plantations in
688 south-central Chile. *Journal of Soil and Water Conservation*, 74(1):12–23, 12 2019. ISSN 0022-4561. doi:
689 10.2489/jswc.74.1.12. URL <http://www.jswconline.org/lookup/doi/10.2489/jswc.74.1.12>.
- 690 M. a. Summerfield and N. J. Hulton. Natural controls of fluvial denudation rates in major world drainage
691 basins. *Journal of Geophysical Research*, 99(B7):13871–13883, 1994. ISSN 0148-0227. doi: 10.1029/
692 94JB00715. URL <http://dx.doi.org/10.1029/94JB00715>.
- 693 J. Syvitski, J. R. Ángel, Y. Saito, I. Overeem, C. J. Vörösmarty, H. Wang, and D. Olago. Earth's sediment
694 cycle during the Anthropocene. *Nature Reviews Earth & Environment*, 2 2022. ISSN 2662-138X. doi:
695 10.1038/s43017-021-00253-w. URL <https://www.nature.com/articles/s43017-021-00253-w>.
- 696 V. Tolorza, S. Carretier, C. Andermann, F. Ortega-Culaciati, L. Pinto, and M. Mardones. Contrasting
697 mountain and piedmont dynamics of sediment discharge associated with groundwater storage variation
698 in the Biobío river. *Journal of Geophysical Research: Earth Surface*, 119(12):2730–2753, 2014. ISSN
699 21699003. doi: 10.1002/2014JF003105. URL <http://dx.doi.org/10.1002/2014JF003105><http://doi.wiley.com/10.1002/2014JF003105>.
- 701 V. Tolorza, C. H. Mohr, S. Carretier, A. Serey, S. A. Sepúlveda, J. Tapia, and L. Pinto. Suspended Sediments
702 in Chilean Rivers Reveal Low Postseismic Erosion After the Maule Earthquake (Mw 8.8) During a Severe
703 Drought. *Journal of Geophysical Research: Earth Surface*, m:2018JF004766, 6 2019. ISSN 2169-9003. doi:
704 10.1029/2018JF004766. URL <https://onlinelibrary.wiley.com/doi/abs/10.1029/2018JF004766>.
- 705 V. Tolorza, D. Poblete-Caballero, D. Banda, C. Little, C. Leal, and M. Galleguillos. An operational method
706 for mapping the composition of post-fire litter. *Remote Sensing Letters*, 13(5):511–521, 5 2022. ISSN
707 2150-704X. doi: 10.1080/2150704X.2022.2040752. URL <https://www.tandfonline.com/doi/full/10.1080/2150704X.2022.2040752>.
- 709 V. Vanacker, F. von Blanckenburg, G. Govers, A. Molina, J. Poesen, J. Deckers, and P. Kubik. Restor-
710 ing dense vegetation can slow mountain erosion to near natural benchmark levels. *Geology*, 35(4):303,
711 2007. ISSN 0091-7613. doi: 10.1130/G23109A.1. URL <http://geology.gsapubs.org/cgi/doi/10.1130/G23109A.1>.
- 713 V. Vanacker, M. Guns, F. Clapuyt, V. Balthazar, G. Tenorio, and A. Molina. Spatio-temporal patterns
714 of landslides and Erosion in tropical Andean catchments. *Pirineos*, 175, 2020. ISSN 19884281. doi:
715 10.3989/PIRINEOS.2020.175001.

716 V. Vanacker, A. Molina, M. Rosas-Barturen, V. Bonnesoeur, F. Román-Dañobeytia, B. F. Ochoa-Tocachi,
717 and W. Buytaert. The effect of natural infrastructure on water erosion mitigation in the Andes. *SOIL*, 8
718 (1):133–147, 2 2022. ISSN 2199-398X. doi: 10.5194/soil-8-133-2022. URL <https://soil.copernicus.org/articles/8/133/2022/>.

720 M. Vázquez, S. Ramírez, D. Morata, M. Reich, J. J. Braun, and S. Carretier. Regolith production and
721 chemical weathering of granitic rocks in central Chile. *Chemical Geology*, 446:87–98, 2016. ISSN 00092541.
722 doi: 10.1016/j.chemgeo.2016.09.023. URL <http://dx.doi.org/10.1016/j.chemgeo.2016.09.023>.

723 J. Verbesselt, R. Hyndman, G. Newnham, and D. Culvenor. Detecting trend and seasonal changes in satellite
724 image time series. *Remote Sensing of Environment*, 114(1):106–115, 1 2010. ISSN 00344257. doi: 10.1016/
725 j.rse.2009.08.014. URL <http://linkinghub.elsevier.com/retrieve/pii/S003442570900265X>.

726 F. von Blanckenburg. The control mechanisms of erosion and weathering at basin scale from cosmo-
727 genic nuclides in river sediment. *Earth and Planetary Science Letters*, 237(3-4):462–479, 2005. ISSN
728 0012821X. doi: 10.1016/j.epsl.2005.06.030. URL <http://www.sciencedirect.com/science/article/pii/S0012821X05004139>.

730 F. von Blanckenburg and J. K. Willenbring. Cosmogenic Nuclides: Dates and Rates of Earth-
731 Surface Change. *Elements*, 10(5):341–346, 10 2014. ISSN 1811-5209. doi: 10.2113/gselements.10.
732 5.341. URL <http://elements.geoscienceworld.org/content/10/5/341.abstract><http://elements.geoscienceworld.org/cgi/doi/10.2113/gselements.10.5.341>.

734 J. Wainwright, L. Turnbull, T. G. Ibrahim, I. Lexartza-Artza, S. F. Thornton, and R. E. Brazier. Link-
735 ing environmental régimes, space and time: Interpretations of structural and functional connectivity.
736 *Geomorphology*, 126(3-4):387–404, 2011. ISSN 0169555X. doi: 10.1016/j.geomorph.2010.07.027. URL
737 <http://dx.doi.org/10.1016/j.geomorph.2010.07.027>.

738 E. Wohl, G. Brierley, D. Cadol, T. J. Coulthard, T. Covino, K. A. Fryirs, G. Grant, R. G. Hilton, S. N.
739 Lane, F. J. Magilligan, K. M. Meitzen, P. Passalacqua, R. E. Poepl, S. L. Rathburn, and L. S. Sklar.
740 Connectivity as an emergent property of geomorphic systems. *Earth Surface Processes and Landforms*,
741 44(1):4–26, 1 2019. ISSN 01979337. doi: 10.1002/esp.4434. URL <http://doi.wiley.com/10.1002/esp.4434>.

743 Y. Zhao, D. Feng, L. Yu, X. Wang, Y. Chen, Y. Bai, H. J. Hernández, M. Galleguillos, C. Estades,
744 G. S. Biging, J. D. Radke, and P. Gong. Detailed dynamic land cover mapping of Chile: Accuracy
745 improvement by integrating multi-temporal data. *Remote Sensing of Environment*, 183:170–185, 9 2016.
746 ISSN 00344257. doi: 10.1016/j.rse.2016.05.016. URL <http://linkinghub.elsevier.com/retrieve/pii/S0034425716302188>.

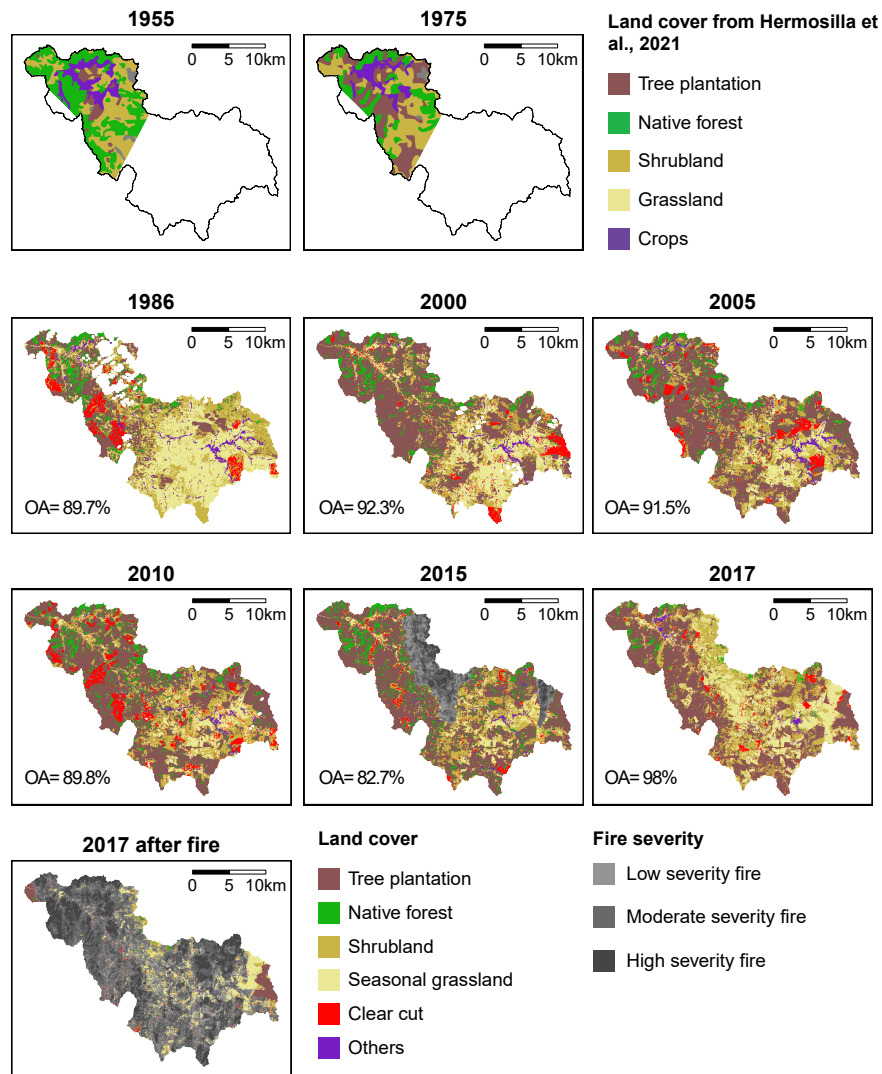
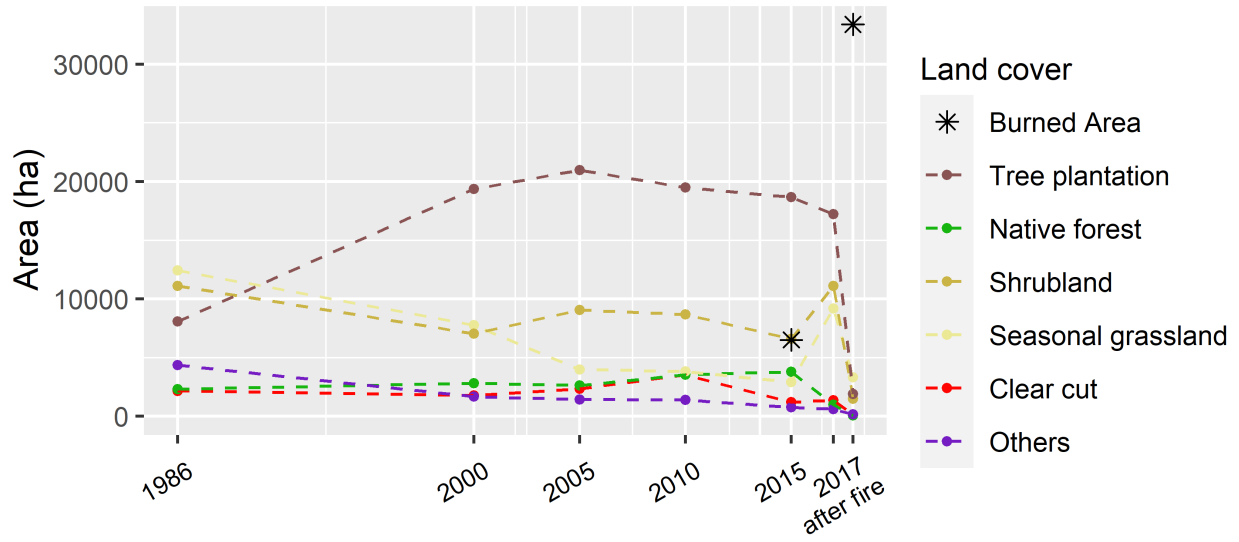


Figure 6: Land cover classification and transitions. Maps of 1955 and 1975 from Hermosilla-Palma et al. (2021), 1986-2015 from this work, and 2017 from Tolorza et al. (2022).

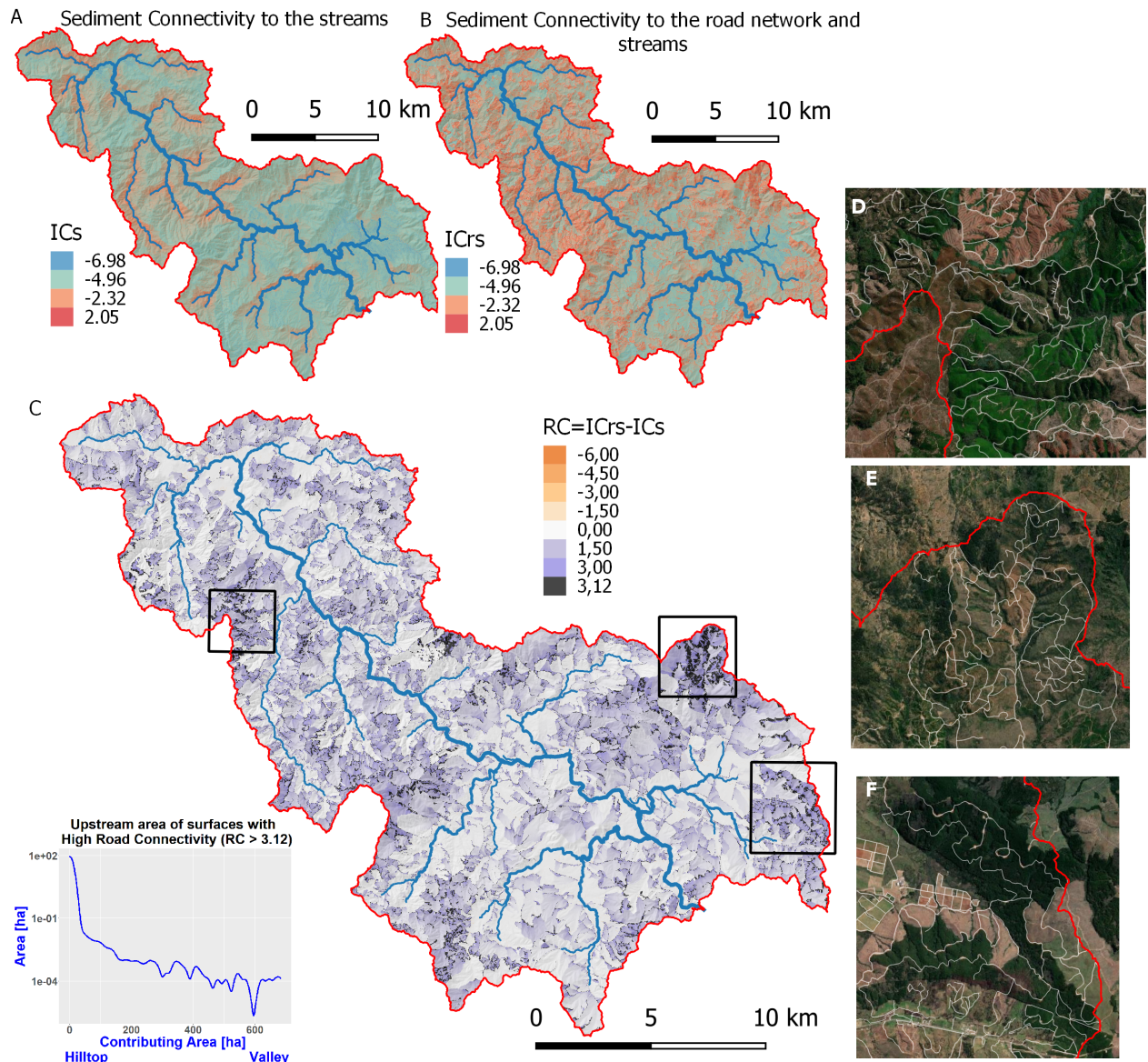


Figure 7: Sediment connectivity index (Cavalli et al., 2013) calculated using (A) the streams and (B) the streams and forest roads as targets. (C) is the difference between both models. (D-F) Details of hilltops with highest values of RC .

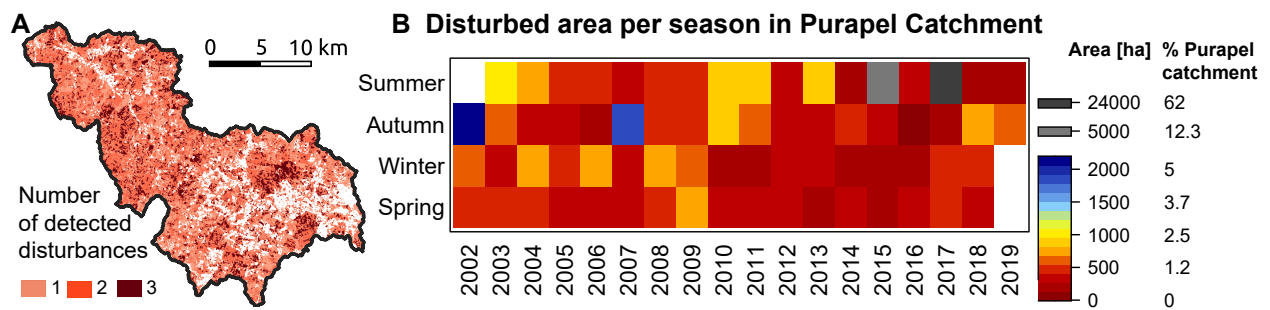


Figure 8: Detected disturbances from BFAST (A) map of the number of disturbances in vegetation detected for the period 2002-2019 (B) Seasonality of disturbance area detected within the Purapel catchment.